Chip Level Decision Feedback Equalizer for CDMA Downlink Channel

Agus Santoso
B.E.

A thesis submitted in fulfillment of the
requirements for the degree of
Master of Engineering Science

School of Electrical and Electronic Engineering
The University of Adelaide
Australia

October 2003

Declaration

The research work in this thesis, submitted for the degree of Master of Engineering Science by Research, was undertaken at the School of Electrical and Electronic Engineering, the University of Adelaide, Australia, under the supervision of Assoc. Prof. Cheng Chew Lim and Dr. Jinho Choi.

This thesis comprises my original work, and to the best of my knowledge does not contain any material written or published by another person except where appropriate acknowledgement has been made in the text. This thesis has not been submitted for any other degree or award at any university or other education institute.

Agus Santoso
October, 2003

Acknowledgements

I would like to express my deep gratitude and appreciation to my supervisors, Assoc. Prof. Cheng Chew Lim and Dr. Jinho Choi, for their valuable guidance, ideas, insight, time and encouragement throughout the project. Without their encouragement and time, the work undertaken would have been impossible to complete.

I also deeply appreciate Prof. Branka Vucetic for her constant help and constructive comments. In addition, I would like to thank Dr. Predrag Rapajic and Joe Yiu for their support during my stay in The University of New South Wales.

I am grateful for the financial support from the University of Adelaide through the provision of the Adelaide University Postgraduate Research Award.

I would like to thank Miss Mia Hadikusuma for her continued understanding throughout many difficult times.

Obviously, my parents, my brothers, and my sisters, thank you for your unconditional love and trust. Without all of you, I would have not become what I am now.

Most importantly, I would like to praise my righteous and merciful God, Jesus Christ, for leading and helping me all the way in my life, especially during my toughest time.

The LORD is my shepherd, I shall not be in want. He makes me lie down in green pastures, He leads me beside quiet waters, He restores my soul. He guides me in paths of righteousness for His name's sake. Even though I walk through the valley of the shadow of death, I will fear no evil, for You are with me; Your rod and Your staff, they comfort me (Psalm 23).

Abstract

In most commercial wideband code division multiple access (W-CDMA) systems, the transmitted signal in the downlink channel is spread by orthogonal codes to accommodate different users. However, frequency selective fading destroys the orthogonality and causes multiple access interference (MAI).

The rake receiver has been proposed for a receiver in the downlink channel. Although providing reasonable performance due to path diversity, the rake receiver does not restore the orthogonality. As a result, the MAI is still present at the output of the rake receiver and CDMA system becomes an interference limited system. Thus, a better approach to provide MAI suppression shall be considered.

The chip level linear equalizer followed by a despreader is an attractive alternative receiver to restore the orthogonality and to suppress the MAI. However, the performance of the chip level linear equalizer depends on the spectral characteristic of the channel and may not be satisfactory for some channels. To overcome this difficulty, the chip level decision feedback equalizer can be used.

To improve the performance further, multiple-input multiple-output (MIMO) channels by using multiple antennas can also be employed. Recent research in information theory shows that multiple antennas can mitigate multipath fading in a wireless channel, increase the information capacity of wireless communication systems dramatically, and improve the reliability of the communications over wireless channel.

In this thesis, the chip level decision feedback equalizer for CDMA downlink channel with multiple antennas is investigated. The work includes the design of the chip level decision feedback equalizer when the space time spreading scheme and the Alamouti scheme are employed at the transmitter. Theoretical and simulation results show significant performance gains compared to the rake receiver and the chip level linear equalizer.

List of Abbreviations

AMPS	Advanced Mobile Phone Service
AWGN	Additive White Gaussian Noise
BER	Bit Error Rate
CDMA	Code Division Multiple Access
CSI	Channel State Information
DFE	Decision Feedback Equalizer
DS-CDMA	Direct-Sequence CDMA
FDD	Frequency Division Duplexing
FDMA	Frequency Division Multiple Access
FIR	Finite Impulse Response
GSM	Global System for Mobile Communication
ICI	Interchip Interference
i.i.d.	Independent and Identical Distributed
ISI	Intersymbol Interference
IS-95	Interim Standard 95
LE	Linear Equalizer
LMMSE	Linear Minimum Mean Square Error
LMS	Least Mean Square
MAI	Multiple Access Interference
MIMO	Multiple-Input Multiple-Output
MRC	Maximal Ratio Combining
MSE	Mean Square Error

MSEG	Mean Square Error Gradient
NLMS	Normalized Least Mean Square
QPSK	Quadrature Phase Shift Keying
RLS	Recursive Least Square
SG	Stochastic Gradient
SNR	Signal to Noise Ratio
ST	Space Time
STS	Space Time Spreading
STTD	Space Time Transmit Diversity
STTC	Space Time Trellis Code
TDD	Time Division Duplexing
TDMA	Time Division Multiple Access
TD-SCDMA	Time Division-Synchronous CDMA
W-CDMA	Wideband CDMA
ZF	Zero Forcing

List of Principal Symbols

$\mathbf{x}$	vector $\mathbf{x}$
$\mathbf{X}$	matrix $\mathbf{X}$
$\mathbf{X}^T$	transpose of matrix $\mathbf{X}$
$\mathbf{X}^H$	Hermitian transpose of matrix $\mathbf{X}$
$\mathbf{X}^*$	complex conjugate of matrix $\mathbf{X}$
$\mathbf{X}^{-1}$	inverse of matrix $\mathbf{X}$
$(\mathbf{X})_k$	the kth row of matrix $\mathbf{X}$
$(\mathbf{X})_{k:l}$	row k up to l of matrix $\mathbf{X}$
$\|\mathbf{X}\|$	Frobenius norm of matrix $\mathbf{X}$
$\mathbf{0}$	zero matrix
$\mathbf{I}$	identity matrix
$\hat{x}$	estimate of x
$\tilde{x}$	hard estimate of x
$\|x\|$	absolute value of x
$\nabla_{\mathbf{x}}$	gradient with respect to vector $\mathbf{x}$
h_{ji}	channel from transmit antenna i to receive antenna j
$e[m]$	a posteriori estimation error signal
$\varepsilon[m]$	a priori estimation error signal
$\eta[m]$	noise signal
$x_k^i[m]$	the mth symbol from transmit antenna i to user k
$E(\cdot)$	expectation function
$\delta(\cdot)$	Dirac delta function

Contents

List of Figures

Chapter 1

Introduction

In the last few years, there has been a rapidly growing interest in wireless technology. Compared to wired technology, wireless technology gives freedom of movement for the users and helps eliminate ineffective calls experienced with the fixed telephone service when the user is away from the terminal. In addition, wireless technology offers more timeliness, affordability, and efficiency. If rivers, freeways or other obstacles stand in the way of a connection, a wireless solution may be much more economical and feasible than installing physical cable [1].

In order to provide the wireless services to subscribers over a certain region with limited spectrum resource, a cellular structure is employed [2]. The cellular structure of wireless systems requires a base station to be placed in each cell. Moving subscribers can communicate with other moving subscribers through base stations in any places. Therefore, there exists communication from the base station to the subscribers, called the downlink (forward link) and the communication from the subscribers to the base station, called the uplink (reverse link). The two directions of communication can be separated in frequency, called frequency division duplexing (FDD), or can be separated in time, called time division duplexing (TDD).

In both downlink and uplink communications, the limited spectrum resources are shared

among users using multiple access techniques. The basic multiple access techniques are frequency division multiple access (FDMA), time division multiple access (TDMA) and code division multiple access (CDMA) [3].

1.1 The Cellular Concept

The cellular concept is the key idea that provides wireless services over regions, countries or continents with a limited spectrum allocation. It is a major breakthrough in solving the problem of spectral congestion and user capacity [2].

In a cellular structure, the coverage region is divided into smaller number of geographic areas called cells, as shown in Fig. 1.1. Each unique cell is assigned with different frequency bands to avoid any co-channel interference. The base station is placed at each unique cell for communication between users within the same cell or for communication between base stations. In each cell, the allocated channel is also divided into many sub-channels and users in a cell use different sub-channels to avoid interference.

Frequency reuse is a major concept to implement the cellular concept. It is used for measuring the efficiency of the system. The ratio of the number of cells using the same frequency band over the total number of cells is called the frequency reuse factor. When the frequency reuse factor reaches unity, the system can provide maximum number of channels. In Fig. 1.1, three cells that are denoted by the same letter use the same frequency band. The cellular concept can be utilized in FDMA, TDMA and CDMA systems.

The number of users that a system can accommodate must be traded off with the interference produced in the system. If the channel cell reuse increases and approaches the unity frequency reuse factor, the total channel available in the system will increase. Thus, more users can be accommodated in the system. However, the interference will be more significant.

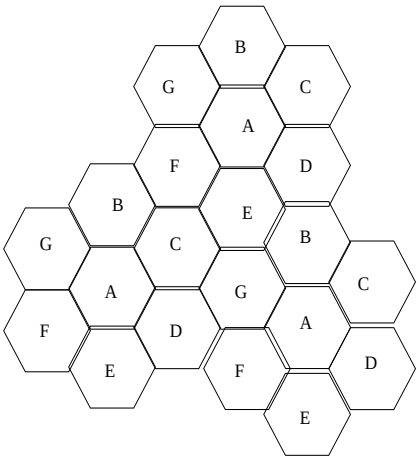

Figure 1.1: Illustration of the cellular frequency reuse concept involving 7 cells

1.2 Multiple Access Principles

In each cell, the available bandwidth is shared among users. The different multiple access schemes determine the different ways users access the available bandwidth [3]. Fig. 1.2 shows the basic multiple access techniques. Note that each block represents each user within the same cell.

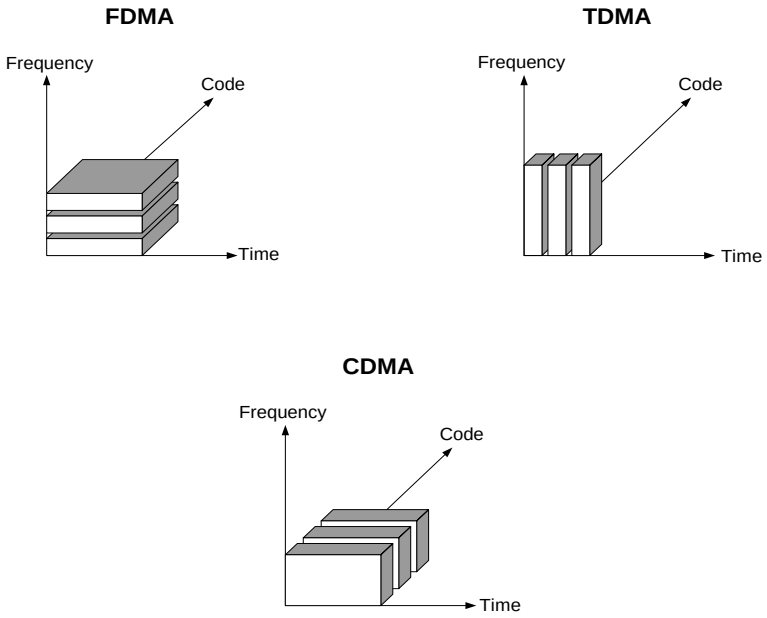

Figure 1.2: Basic multiple access techniques

The first generation of wireless system, advanced mobile phone service (AMPS) uses FDMA system for accessing the available spectrum resource. In FDMA system, each user within the same cell operates in an unique frequency channel. As a result, there is no intra-cell interference.

The second generation system based on global system for mobile communication (GSM) uses a combination of FDMA and TDMA systems [4]. TDMA system allows each user within the same cell to operate in an unique time channel. Each frequency in a GSM system has a bandwidth of 200 kHz and is divided into eight time channels.

In 1995, the first CDMA technology for the second generation wireless system, called Interim Standard 95 (IS-95), was commercially launched. CDMA technology has also been adopted as a standard in the third generation wireless system [2]. Wideband CDMA (W-CDMA), time division-synchronous CDMA (TD-SCDMA), and CDMA2000 are the three operating modes in the third generation CDMA system. The direct-sequence CDMA (DS-CDMA) system is one of the most popular CDMA systems used in IS-95 and W-CDMA [5]. In a CDMA system, each user within the same cell operates in the same frequency and time channel.

1.3 Benefits of CDMA Systems

CDMA systems offer numerous advantages over FDMA and TDMA systems [6]. The advantages include:

1. CDMA system provides capacity improvement.
   Frequency reuse factor of CDMA system reaches unity. Therefore, it can accommodate more users within its cell.

2. CDMA technology provides higher data rate transmission.
   The higher data rate transmission can be achieved by spreading information into a wideband signal.

3. CDMA technology provides better handoff in the system.
   CDMA system starts to communicate with a new cell before it crosses the boundary, without dropping the link with the current (old) cell.

4. CDMA system optimizes the channel resource usage.
   For voice transmission, a user is active less than half the time. In FDMA and TDMA systems, where each user is allocated unique frequency or time channel, this causes a great loss in capacity. CDMA system operates in the same frequency and time channel. Thus, this problem does not occur [6].

5. CDMA system suppresses multipath interference more efficiently.
   In the scattering environment, the received signal comes from different paths. Since in a CDMA system each user is assigned with a larger bandwidth than in a FDMA or TDMA system, the different paths are better isolated. Thus, multipath interference can be minimized better than in FDMA or TDMA system.

1.4 Receivers for a CDMA System

Improvement of downlink capacity is one challenge facing the effort toward third generation wireless system. In commercial W-CDMA, the transmitted signal in the downlink channel is spread by orthogonal codes [5]. In a flat fading channel where the propagation delay of multipath signal is negligible, a simple despreader is sufficient to suppress multiple access interference (MAI) resulting from the effects of the interference from other users within a cell. However, once we have a frequency selective fading channel, the orthogonality cannot be retained. Therefore, MAI exists at the output of the despreader and the performance degrades.

One can design a receiver to improve the performance by mitigating multipath fading for the CDMA downlink channel. For example, the rake receiver can be used to get path diversity [7]. Although the rake receiver can provide reasonable performance due to path diversity, its performance is still limited by MAI, the numbers of multipaths, power control in the

downlink channel, and channel estimation error. Consequently, better approaches such as MAI suppression shall be considered.

Many innovative receivers have been proposed to suppress MAI. Multiuser detection techniques that use joint code, timing and channel information can be employed to improve performance by mitigating MAI [8–11]. Although multiuser detection techniques outperform the rake receiver, the complexity is high. Therefore, it is impractical to apply these techniques in mobile terminals due to computing constraints.

Equalization can be adopted to restore orthogonality without significantly increasing the complexity. Then, a despreader can suppress MAI from the orthogonal signal. The chip level linear equalizer (LE) restores the orthogonality of the chip sequence and performs better than the rake receiver [12–15]. However, if the channel equalization is not perfect, the performance of the chip level LE is degraded by MAI. Moreover, the performance of the chip level LE still depends on the spectral characteristic of the channel and may not be satisfactory for some channels.

When investigating more powerful receiver algorithms, one might consider decision feedback equalizer (DFE). The DFE [16] can have better immunity against spectral channel characteristics, reduce the noise enhancement effect, shorten the length of equalizer tap, and give the forward linear filter greater flexibility in handling intersymbol interference (ISI) resulting from the interference from other symbols at the sampling instant. Thus, the DFE outperforms the LE. The standard DFE for nonspread signal has been considered in many papers [17–19]. Chip level DFE for CDMA systems that used short spreading sequences [20, 21] and long spreading sequences [22] has also been studied.

To improve the performance further, multiple-input multiple-output (MIMO) channels (by using multiple antennas) can also be employed [23–25]. MIMO channels can provide additional diversity gain to the mobile station and thus, can improve the performance. Different schemes such as space time spreading [26] and space time transmit diversity [27] were developed to achieve diversity gain in CDMA systems.

Space time spreading (STS) [26] spreads each signal in a balanced way over the transmitter

antenna elements to provide maximal path diversity at the receiver. The simplest STS scheme is when each user is assigned with a different orthogonal code for each transmit antenna.

Space time transmit diversity (STTD) explores the spatial and temporal diversities as well as coding gain to improve the performance of the MIMO system. STTD can provide diversity gain over an uncoded system without sacrificing bandwidth and can increase the effective transmission rate as well as the potential system capacity. Alamouti discovered a remarkable STTD scheme for transmission with two antennas [27]. This scheme was later generalized by Tarokh *et al.* to an arbitrary number of antennas [28]. This generalized scheme is also able to achieve the full diversity promised by any numbers of transmit and receive antennas.

DFE based on the minimum mean square error (MMSE) criterion [19] for nonspread signals in multiple antennas has been derived in literatures [29–31]. MMSE-DFE has better performance when compared to the MMSE-LE, especially with the highly dispersive and nonminimum phase characteristic channel [30].

These findings have motivated us to design a chip level DFE for CDMA downlink channel with multiple antennas. The design of the chip level DFE for CDMA downlink channel in multiple antennas is not straightforward and offers numerous challenges. The first challenge is to develop a method to provide the chip feedback from the symbol decision. The second challenge is to find a better way to suppress the interference, both from other users and other transmit antennas. In the MIMO CDMA system, interferences do not only originate from past symbols of the desired user, but also from current symbols and past symbols of other (interfering) users and antennas. The third challenge is to develop a method to detect signals buried in interchip interference (ICI), in addition to noise. The ICI is defined as the interference between chips caused by frequency selective fading channels.

Note that the MMSE-LE for CDMA downlink channel in multiple antennas, i.e. the space time chip level LE, has also been proposed [32, 33]. The space time chip level LE is less affected by the channel estimation error and thus, can have better performance compared to the space time rake receiver with estimated channel. However, the space time chip level LE still has comparable performance to the space time rake receiver with perfect channel state

information (CSI).

It is important to stress that the analysis of the DFE is difficult due to their inherent nonlinear nature. Only by assuming that past decisions are correct, the problem can be linearized and MMSE solutions formulated.

This thesis deals with the chip level DFE designs for CDMA downlink channel when multiple antennas are used.

1.5 Outline of the Thesis

This thesis is organized into five chapters. Chapter 2 gives basic concepts about the principal of communication channel and the model for time-variant multipath signal propagation. The standard DFE receiver for nonspread signal is discussed, and the optimum equalizer coefficients and the MMSE solution are derived. This chapter also discusses three adaptation algorithms: least mean square, normalized least mean square, and recursive least square algorithms. The mathematical description of the spreading operation for the DS-CDMA system, including the signal model for DS-CDMA MIMO downlink channel, is presented. The rake receiver and the chip level LE for a DS-CDMA system are reviewed.

There are two major parts in Chapter 3. In the first part, we develop a new chip level DFE for CDMA downlink channel when the STS is employed at the transmitter. In the second part, we present a new chip level DFE design when the Alamouti transmit diversity scheme is employed at the transmitter. The optimum solution for the Alamouti scheme is derived and analyzed. In both parts, the adaptive implementation is presented.

Simulation results and performance comparison of different receivers design are presented in Chapter 4. We investigate the effect of different adaptation algorithms and different transmission schemes on the bit error rate (BER) performance.

Chapter 5 summarizes the main findings and gives some suggestions for further research.

1.6 Publications

The publications related to the thesis are as follows.

1. Agus Santoso, Jinho Choi and Cheng Chew Lim,“Multiple input multiple output chip level decision feedback equalizer for CDMA downlink channel,” in *Proceedings of the Fourth Australasian Workshop on Signal Processing and Applications*, Brisbane, Australia, Dec 2002, pp. 151-154.

2. Agus Santoso, Jinho Choi, Cheng Chew Lim and Branka Vucetic,“A chip level decision feedback equalizer for CDMA downlink channel with the Alamouti transmit diversity scheme,” in *Proceedings of the IEEE International Symposium on Personal, Indoor and Mobile Radio Communications*, Beijing, China, Sept 2003, pp. 1322-1326.

3. Agus Santoso, Jinho Choi, Cheng Chew Lim and Branka Vucetic,“Chip level decision feedback equalizer for CDMA downlink channel with space-time coding,” *Electronics Letters*, accepted for publication.

Chapter 2

Fundamental Concepts

This chapter discusses the fundamental concepts of the communication channel model, the standard decision feedback equalizer (DFE) for a nonspread signal, and three adaptation algorithms. In addition, this chapter gives the basic principle of DS-CDMA system, describes the general signal model for CDMA MIMO downlink channel, and reviews receiver structures of the rake receiver and the chip level linear equalizer for a DS-CDMA downlink channel.

2.1 Communication Channel Model

The communication system involves the transmission of information from one place to another through the medium (channel). Fig. 2.1 illustrates the functional diagram and the basic elements of a communication system [19].

The propagation of the signal on both downlink and uplink is affected by a channel in several ways. For a multipath channel, the propagation results in the spreading of the signal in three dimensions. These are the delay (time) spread, Doppler (frequency) spread, and angle spread [34]. Depending on the amount of the delay spread and the Doppler spread, the various fading can be categorized as shown in Fig. 2.2.

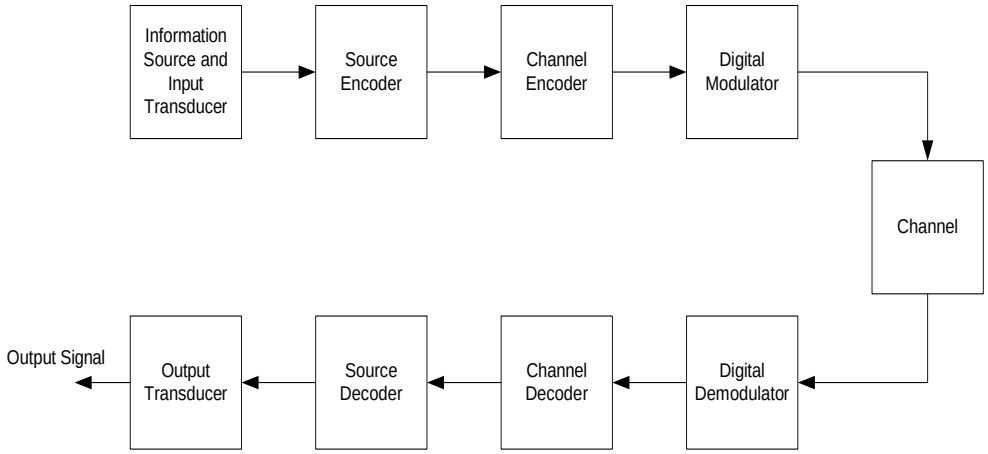

Figure 2.1: The basic elements of a communication system

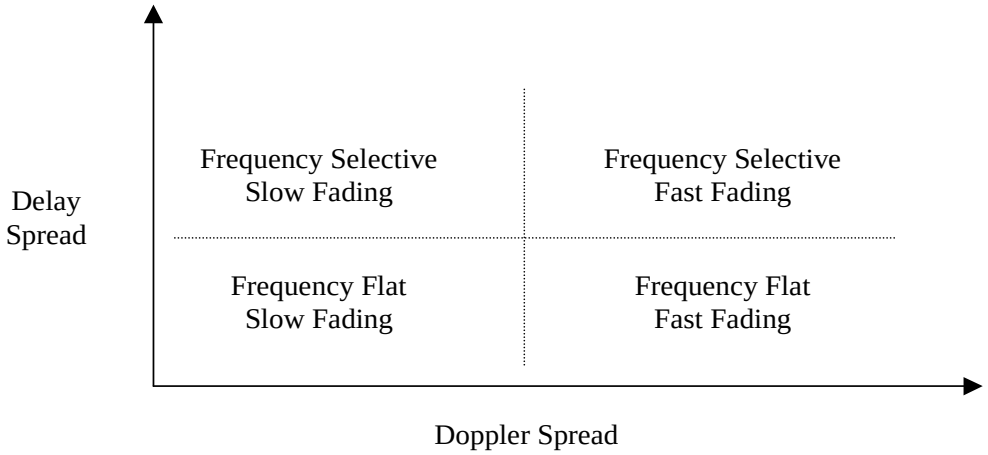

Figure 2.2: Fading categories based on delay spread and Doppler spread

Delay spread is caused by the multipath because of remote scatterers such as hills or terrains. As a result, several time-shifted and time-scaled versions of the transmitted signal will arrive at the receiver. Delay spread causes frequency selective fading, and can be measured in terms of coherence bandwidth. The larger delay spread, the smaller coherence bandwidth. Depending on the coherence bandwidth, a channel can be categorized into frequency nonselective (flat) fading channel or frequency selective fading channel.

Doppler spread is caused by mobile motion and local scattering near the mobile. Doppler spread causes time selective fading and can be characterized by the coherence time of the channel. The larger Doppler spread, the smaller the coherence time, and the faster the chan-

nel characteristics vary with time. Thus, from Doppler spread, a channel can be categorized into fast fading (high Doppler spread) or slow fading channel (low Doppler spread).

Angle spread is the spread of arrival (or departure) angles of the multipath at the antenna array. The angle of arrival (or departure) of a path can be statistically related to the path delay. Angle spread results from remote scatterers and local scattering near the base station. Angle spread causes space selective fading and can be characterized by the coherence distance. The larger the angle spread, the shorter the coherence distance.

Let $h_{ji}(t)$ denote the continuous time impulse response of the multipath channel from transmit antenna i to receive antenna j. A time-variant multipath signal propagation through the mobile cellular radio channel can be modelled as:

$$h_{ji}(t) = \sum_{p=0}^{P-1} \alpha_{ji,p}(t) e^{j\theta_{ji,p}(t)} \delta(t - \tau_{ji,p}(t)) \tag{2.1}$$

where P is the number of channel multipath, $\delta(\cdot)$ is the Dirac delta function, and $\alpha_{ji,p}(t)$, $\theta_{ji,p}(t)$, and $\tau_{ji,p}(t)$ are the time-variant attenuation, phase distortion, and propagation delay of the pth path from transmit antenna i to receive antenna j, respectively.

Note that the propagation delay $\tau_{ji,p}(t)$ characterizes different multipaths (delay spread), and the time-variant attenuation and the phase distortion characterize the amount of the Doppler spread.

2.2 Standard Decision Feedback Equalizer (DFE)

We first describe the standard decision feedback equalizer (DFE) receiver for a nonspread signal, upon which chip level DFE for DS-CDMA system builds. A DFE is a nonlinear equalizer that employs previous decisions to eliminate the intersymbol interference (ISI) caused by previously detected symbols on the current symbol to be detected.

The standard DFE for a nonspread signal was first suggested by Austin [16]. Fig. 2.3 shows a discrete time complex baseband model for the standard DFE.

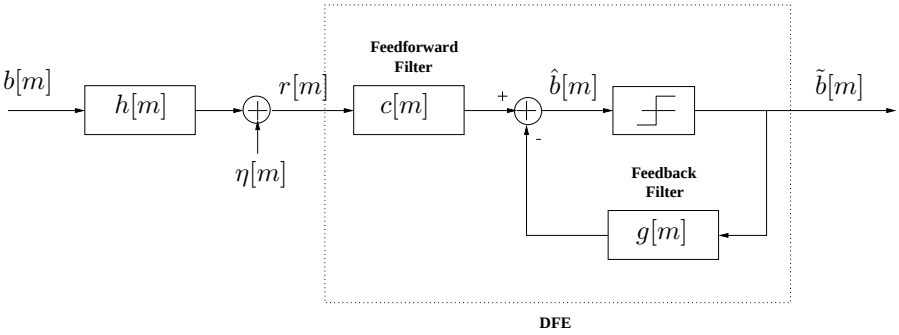

Figure 2.3: The conventional DFE structure for a nonspread signal

The DFE consists of a feedforward filter $c[m]$ and a feedback filter $g[m]$, where m is the symbol index. Because the feedback filter sits in a feedback loop, it must be strictly causal.

The signal propagates through a discrete time-variant frequency selective fading channel $h[m]$. Let P be the number of channel multipath, and the complex channel is assumed time-invariant, i.e. $h[p;m] = h[p]$ for $p = 1, \ldots, P$. The received signal $r[m]$ can be written as:

$$r[m] = \sum_{p=0}^{P-1} h^*[p]b[m-p] + \eta[m] \tag{2.2}$$

where $b[m]$ is the transmitted symbols information, $\{h[p]\}$ is the discrete channel impulse response, $\eta[m]$ is the additive white Gaussian noise with mean zero and variance σ_n^2, and * is the complex conjugate operator.

Let $v[m]$ be the impulse response of the discrete composite system with the channel and feedforward equalizer. That is,

$$v[m] = \sum_{p=0}^{P-1} h^*[p]c[m-p]. \tag{2.3}$$

From Fig. 2.3, the output of DFE can be written as:

$$\hat{b}[m] = \sum_{l=-N_f}^{N_b} v^*[l]b[m-l] - \sum_{l=1}^{N_b} g^*[l]\tilde{b}[m-l] + \bar{\eta}[m] \tag{2.4}$$

where $\tilde{b}[m]$ is the detected symbols, N_f+1 is the length of feedforward taps, N_b is the length of feedback taps, and

$$\bar{\eta}[m] \;=\; \sum_{l=-N_f}^{0} c^*[l]\eta[m-l]. \tag{2.5}$$

Assume that no decision errors are made, i.e. $\tilde{b}[m-l] = b[m-l]$ and $\{g[l]\} = \{v[l]\}$ for $1 \le l \le N_b$, (2.4) can be rewritten as:

$$\hat{b}[m] = \sum_{l=-N_f}^{0} v^*[l]b[m-l] + \bar{\eta}[m]. \tag{2.6}$$

From (2.4) and (2.6), the minimum mean square error (MMSE) can be obtained when the feedforward filter is used to eliminate the ISI from some "future" symbols (precursor ISI), and minimize the noise. The feedback filter, on the other hand, is used to eliminate the ISI from past symbols (postcursor ISI). Note that the cancellation of the postcursor ISI using the feedback filter does not enhance noise, since any noise present is eliminated by the decision device (assuming no decision errors are made). Therefore, there is no noise at the output of the feedback filter. Thus, removing only precursor ISI using a feedforward filter does not enhance noise as much as removing both the precursor and postcursor ISI [35]. The DFE based on the mean square error (MSE) criterion was first investigated by Salz [17].

From (2.4) and (2.6), the output of DFE can also be written:

$$\hat{b}[m] \;=\; \sum_{l=-N_f}^{0} c^*[l]r[m-l] - \sum_{l=1}^{N_b} g^*[l]b[m-l]. \tag{2.7}$$

Let $\mathbf{c}$ and $\mathbf{g}$ be the vector of feedforward and feedback taps, respectively. Let $\mathbf{r}[m]$ and $\mathbf{b}[m]$ be the received signal vector and past detected symbol vector, respectively. That is,

$$\mathbf{c} \;=\; \Big(c[-N_f] \;\; \ldots \;\; c[0]\Big)^T \tag{2.8}$$

$$\mathbf{g} \;=\; \Big(g[1] \;\; \ldots \;\; g[N_b]\Big)^T \tag{2.9}$$

$$\mathbf{r}[m] \;=\; \Big(r[m+N_f] \;\; \ldots \;\; r[m]\Big)^T \tag{2.10}$$

$$\mathbf{b}[m] \;=\; \Big(b[m-1] \;\; \ldots \;\; b[m-N_b]\Big)^T \tag{2.11}$$

where T is the transpose operator.

Let $\mathbf{w}$ be the complete equalizer vector and $\mathbf{d}[m]$ be the complete received vector. That is,

$$\mathbf{w} = \begin{pmatrix} \mathbf{c}^T & \mathbf{g}^T \end{pmatrix}^T \tag{2.12}$$

$$\mathbf{d}[m] = \begin{pmatrix} \mathbf{r}^T[m] & -\mathbf{b}^T[m] \end{pmatrix}^T. \tag{2.13}$$

Thus, (2.7) can be written as:

$$\hat{b}[m] = \begin{pmatrix} \mathbf{c}^H & \mathbf{g}^H \end{pmatrix} \begin{pmatrix} \mathbf{r}[m] \\ -\mathbf{b}[m] \end{pmatrix} \tag{2.14}$$

$$\hat{b}[m] = \mathbf{w}^H \mathbf{d}[m] \tag{2.15}$$

where H is the Hermitian transpose operator.

The weight vector $\mathbf{w}$ is chosen to minimize the mean square error (MSE) as:

$$MSE = E\Big(|b[m] - \hat{b}[m]|^2\Big). \tag{2.16}$$

Assume that the noise sequence and the symbol sequence are uncorrelated. The optimal solution for the conventional DFE under the MMSE criterion is

$$\mathbf{g} = \mathbf{H}\mathbf{c} \tag{2.17}$$

$$\mathbf{c} = (\bar{\mathbf{H}}^H \bar{\mathbf{H}} + \sigma_n^2 \mathbf{I})^{-1} \mathbf{h}_c^* \tag{2.18}$$

where

$$\mathbf{h}_c = \begin{pmatrix} h[N_f] & h[N_f - 1] & \dots & h[0] \end{pmatrix}^T \tag{2.19}$$

$$\mathbf{H} = \begin{pmatrix} h[N_f + 1] & \dots & h[2] & h[1] \\ \vdots & & \vdots & \vdots \\ 0 & & h[N_b] & h[N_b - 1] \\ 0 & \dots & 0 & h[N_b] \end{pmatrix} \tag{2.20}$$

$$\bar{\mathbf{H}} = \begin{pmatrix} h[0] & 0 & \dots & 0 \\ h[1] & h[0] & & 0 \\ \vdots & \vdots & \ddots & \vdots \\ h[N_f] & h[N_f-1] & \dots & h[0] \end{pmatrix} \tag{2.21}$$

and $\mathbf{I}$, $h[p]$ are the identity matrix and the discrete time of the pth path channel, respectively.

Proof: See Appendix A.

In addition, the MMSE solution is given as:

$$MMSE = 1 - \mathbf{h}_c^T(\bar{\mathbf{H}}^H\bar{\mathbf{H}} + \sigma_n^2\mathbf{I})^{-1}\mathbf{h}_c^*. \tag{2.22}$$

Note that the MMSE solution and the optimal equalization vector in terms of matrix formulation are not discussed by Austin and Salz [16, 17].

Although the conventional DFE performs better than the linear equalizer, any decision errors at the output of the decision device are propagated by the feedback filter. This error propagation has been explored and the benefit of reduced noise enhancement usually far outweighs the effect of error propagation [36].

2.3 Adaptation Algorithms

The optimum solution for the tap equalizer in (2.17) and in (2.18) can be found analytically by solving matrix inversion directly. The solution can also be found iteratively by using mean square error gradient (MSEG) algorithm. Although both methods are quite straightforward, they require the knowledge of the channel property in advance. In addition, to solve the optimum solution iteratively, the channel must be time-invariant. In most communication systems that employ equalizers, we cannot predict the channel accurately since the channel characteristics are unknown a priori, and in many cases, the channel response is time-variant. Therefore, the prediction of the channel is difficult in the fast fading channel and an adaptation algorithm is needed.

In any adaptation algorithms, the equalizer can automatically track and modify its equalizer coefficients to compensate for the time variations in the channel response. The choice of the adaptation algorithm can greatly influence the system performance. The availability of the continuous pilot signal in the third generation system [5] enables the continuous updates of the equalizer coefficients to track the channel variations in a fast fading channel. Since the equalizer is implemented in the mobile station, any adaptation algorithm used must have low computational requirement and fast convergence rate. The least mean square (LMS) algorithm, the normalized least mean square (NLMS) algorithm, and the recursive least square (RLS) algorithm are well suited for such applications.

2.3.1 Least Mean Square Adaptation Algorithm

The least mean square (LMS) adaptive transversal filter or stochastic gradient (SG) algorithm can track the channel variation and can modify the equalizer coefficients. Transmission of the pilot signal is needed to adjust the equalizer coefficients.

The SG algorithm [36] takes the form:

$$\hat{\mathbf{w}}[m+1] = \hat{\mathbf{w}}[m] - \frac{\mu}{2}\nabla_{\mathbf{w}}(|e[m]|^2)\Big|_{\mathbf{w}=\mathbf{w}[m]} \tag{2.23}$$

where μ is the step size or adaptation gain, $\nabla_{\mathbf{w}}$ is the gradient with respect to $\mathbf{w}$, $e[m]$ is the a posteriori estimation error signal, $\hat{\mathbf{w}}[m]$ is the equalizer vector, and $\hat{\mathbf{w}}[m+1]$ is its update.

If $|e[m]|^2$ is expanded and differentiated with respect to the equalizer coefficients, we may obtain the results in the form of three basic relations as follows [37]:

$$\hat{b}[m] = \hat{\mathbf{w}}^H[m]\mathbf{d}[m] \tag{2.24}$$

$$e[m] = \bar{b}[m] - \hat{b}[m] \tag{2.25}$$

$$\hat{\mathbf{w}}[m+1] = \hat{\mathbf{w}}[m] + \mu e^*[m]\mathbf{d}[m] \tag{2.26}$$

where $\hat{b}[m]$ is the equalizer output, $\mathbf{d}[m]$ is the tap-input vector, and $\bar{b}[m]$ is the desired (pilot) signal.

The LMS adaptation algorithm is simple and easy to implement. It requires low computational complexity and it serves as a basis for the derivation of a number of other algorithms. From (2.24)-(2.26), we can see that the LMS algorithm requires only 2κ complex multiplications and $2\kappa + 1$ complex additions per iteration, where κ is the number of tap weights used in the adaptive filter. In other words, the computational complexity of the LMS algorithm is only $O(\kappa)$. However, the LMS algorithm has a relatively slow convergence rate.

2.3.2 Normalized Least Mean Square Adaptation Algorithm

From the standard LMS algorithm in (2.26), the correction factor of each iteration is directly proportional to the tap input vector $\mathbf{d}[m]$. Therefore, when $\mathbf{d}[m]$ is large, the LMS algorithm may experience a gradient noise amplification problem. To deal with this problem, the normalized least mean square (NLMS) adaptation algorithm as a modification of the LMS algorithm is used. In addition, the NLMS algorithm also provides faster convergence rate than the LMS algorithm with a relatively small increase in algorithm complexity. The term "normalized" in the NLMS algorithm refers to the correction factor at each iteration normalized with respect to the square Euclidean norm of the tap input vector $\mathbf{d}[m]$.

From the same cost function in (2.16), the NLMS algorithm can be written as:

$$\hat{\mathbf{w}}[m+1] = \hat{\mathbf{w}}[m] + \frac{\bar{\mu}}{a + \|(\mathbf{d}[m])\|^2} e^*[m]\mathbf{d}[m] \tag{2.27}$$

where a is a positive constant and $\bar{\mu}$ is the adaptation constant. Note that the adaptation constant $\bar{\mu}$ for the NLMS algorithm is dimensionless. It must satisfy $0 < \bar{\mu} < 2$ in order to converge in the mean square error [37].

2.3.3 Recursive Least Square Adaptation Algorithm

When faster convergence rate is required, more advanced adaptation algorithms such as the recursive least square (RLS) algorithm can be used. The RLS algorithm has an order of

magnitude faster convergence rate and smaller misadjustment than the LMS and the NLMS algorithms. Therefore, the algorithm can improve the bit error rate (BER) performance. This improvement, however, is achieved at the expense of increasing computational complexity and storage requirements. The computation complexity of the RLS algorithm is $O(\kappa^2)$, where κ is the number of tap weights used in the adaptive filter.

In the RLS algorithm, the computation is started with known initial conditions, and uses the information contained in new data samples to update the old estimates. As a result, the length of observable data is a variable.

The RLS algorithm is designed to minimize the exponentially weighted least squares cost function ξ [37], as:

$$\xi[m] = \sum_{i=1}^{m} \beta(m,i)|\varepsilon[i]|^2 \tag{2.28}$$

where $\varepsilon[i]$ is the ith of the a priori estimation error signal, m is the duration of the observable interval, and $\beta(m,i)$ is the weighting factor.

The commonly used weighting is the exponential weighting factor or forgetting factor defined by

$$\beta(m,i) = \lambda^{m-i}, \qquad i = 1, 2, \ldots, m \tag{2.29}$$

where the forgetting factor λ is a positive constant close to, but less than 1.

The inverse of $1-\lambda$ can be used for measuring the memory of the algorithm. When λ equals 1, we have the ordinary method of least squares, and its memory is infinite. With a forgetting factor incorporated, it ensures that the data input in the distant past is "forgotten", so that the algorithm can follow changes in the system and operate in a time-variant environment.

The RLS algorithm [37] can be written as:

$$\mathbf{k}[m] = \frac{\mathbf{P}[m-1]\mathbf{d}[m]}{\lambda + \mathbf{d}^H[m]\mathbf{P}[m-1]\mathbf{d}[m]} \tag{2.30}$$

$$\varepsilon[m] = \bar{b}[m] - \hat{\mathbf{w}}^H[m-1]\mathbf{d}[m] \tag{2.31}$$

$$\hat{\mathbf{w}}[m] = \hat{\mathbf{w}}[m-1] + \varepsilon^*[m]\mathbf{k}[m] \quad (2.32)$$

$$\mathbf{P}[m] = \frac{\mathbf{P}[m-1] - \mathbf{k}[m]\mathbf{d}^H[m]\mathbf{P}[m-1]}{\lambda} \quad (2.33)$$

where $\mathbf{k}[m]$ is the gain vector, $\hat{\mathbf{w}}[m]$ is the equalizer vector, and $\mathbf{P}[m]$ is the inverse correlation matrix.

2.4 DS-CDMA System

DS-CDMA system enables each user to spread the information bearing signal $b(t)$ with rate $1/\mathrm{T}$ into a wideband signal $u(t)$ with rate N/T using specific code information [2, 5, 6, 38]. N is the processing gain and T is the symbol period. Fig. 2.4 (a) and Fig. 2.4 (b) show the time domain and frequency domain representations of the DS-CDMA spreading operation, respectively.

In the time domain, there will be N chip sequence transmissions during symbol period T after the spreading operation, as illustrated in Fig. 2.4 (a). All users then transmit their chip sequence within the same frequency and time channel. Note that the chip period T_c is given as T/N.

The power spectral density of the information bearing signal $S_b(f)$ and the wideband signal $S_u(f)$ are also shown in Fig. 2.4 (b).

The spreading operation using the specific code information at the transmitter is straightforward. The data symbol is modulated by the code signal. This code signal consists of a number of code bits called chips. The resulting chip sequence is then modulated by a carrier. Fig. 2.5 shows the spreading and modulation operation at the transmitter [5].

At the receiver, each data symbol of the desired user is recovered by multiplying the received chip sequence, with the complex conjugate code sequence of the desired user. This is called despreading operation. After demodulation, the original data symbol can be recovered. Fig. 2.6 shows the despreading and demodulation operation at the receiver [5].

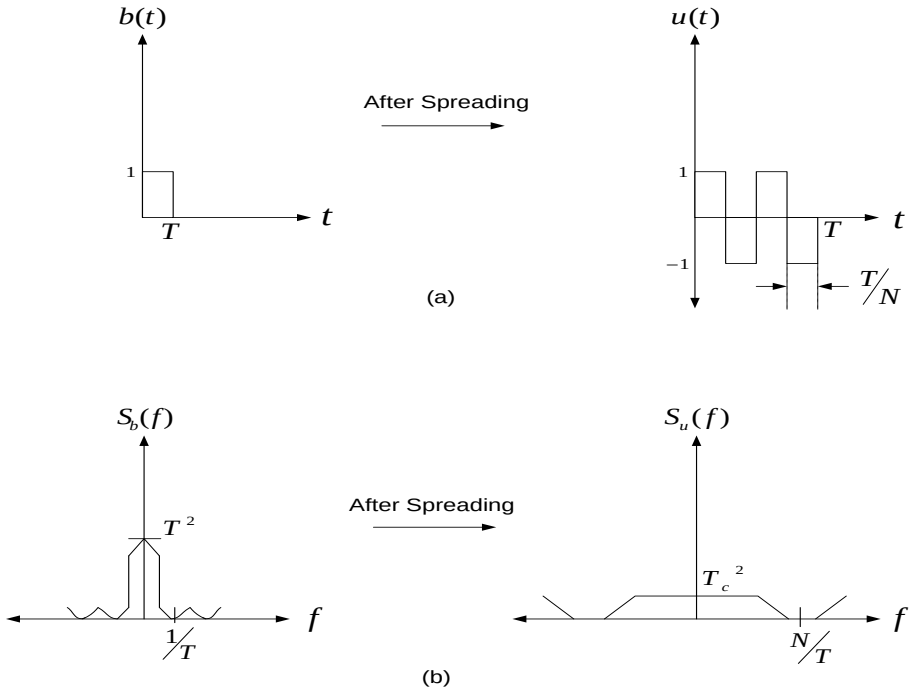

Figure 2.4: The DS-CDMA operation: (a) Time domain representation, (b) Frequency domain representation

For the ideal downlink communication channel, the orthogonality is preserved during the transmission. As a result, a simple despreader receiver is able to suppress all MAI.

To illustrate the ability of a simple despreader to suppress all MAI in the ideal CDMA downlink channel, let us examine an example. Consider the normalized Walsh code with the processing gain $N = 4$. There are 4 users transmitting the single bit symbol synchronously through an ideal downlink channel.

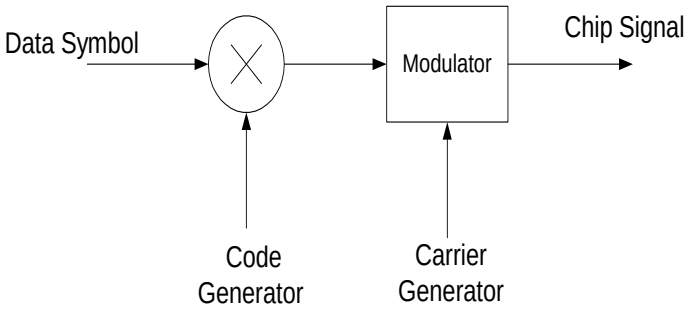

Figure 2.5: The spreading and modulation operation at the transmitter

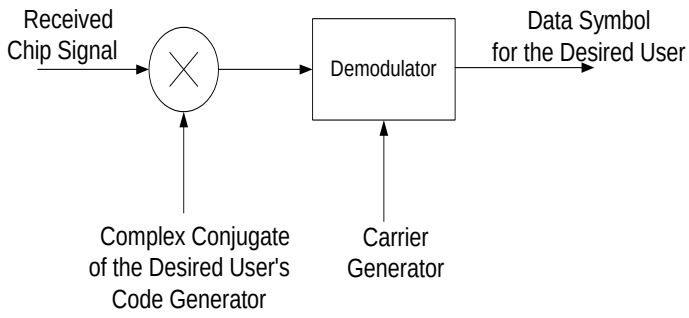

Figure 2.6: The despreading and demodulation operation at the receiver

The normalized Walsh code $\mathbf{s}_k$ and the bit symbol $b_k[m]$ for the 4 users ($k = 1, \ldots, 4$), where m is the symbol index are:

$$\mathbf{s}_1 = \begin{bmatrix} \frac{1}{2} & \frac{1}{2} & \frac{1}{2} & \frac{1}{2} \end{bmatrix}^T, \qquad \mathbf{s}_2 = \begin{bmatrix} \frac{1}{2} & -\frac{1}{2} & \frac{1}{2} & -\frac{1}{2} \end{bmatrix}^T$$
$$\mathbf{s}_3 = \begin{bmatrix} \frac{1}{2} & \frac{1}{2} & -\frac{1}{2} & -\frac{1}{2} \end{bmatrix}^T, \quad \mathbf{s}_4 = \begin{bmatrix} \frac{1}{2} & -\frac{1}{2} & -\frac{1}{2} & \frac{1}{2} \end{bmatrix}^T$$
$$b_1[m] = 1, b_2[m] = -1, b_3[m] = -1, b_4[m] = 1.$$

At the receiver, the received signal vector $\mathbf{r}[n]$ is $[0 \quad 0 \quad 0 \quad 2]^T$, where n is the chip index. If the kth user is the desired user, then by despreading the received signal with respect to the spreading code of the kth user, we can obtain the original information of the bit symbol transmitted by the kth user.

However, the ideal CDMA downlink channel does not exist in practice. A channel introduces noise and a received signal also experiences multipath. Thus, a simple despreader is unable to suppress all MAI. As a result, CDMA becomes an interference limited system and the performance is degraded. Therefore, the different receiver structures for CDMA downlink channel such as the rake receiver and the equalizer are developed to improve the performance.

2.5 Signal Model for a DS-CDMA System

We now develop a general DS-CDMA downlink signal model for multiple antennas. We assume that there are I transmit antennas and J receive antennas with each transmit antenna transmitting a different continuous pilot signal, and there are K users in the system.

Consider the complex baseband model for a downlink channel of a single cell DS-CDMA system. Let $b_k^{(i)}[m]$ be the mth symbol of transmission from transmit antenna i to mobile station k.

The kth user spread signal from transmit antenna i is:

$$\begin{aligned} & u_k^{(i)}[mN+l] = A_k b_k^{(i)}[m] s_k^{(i)}[mN+l] \\ & m = -\infty, \ldots, 0, \ldots, \infty, \quad l = 0, 1, \ldots, N-1, \quad i = 1, 2, \ldots, I \end{aligned} \tag{2.34}$$

where A_k is the amplitude of user k, $s_k^{(i)}[mN+l]$ is the kth user spreading sequence from transmit antenna i, N is the processing gain, m is the symbol index, and l stands for the chip index within a symbol period. Note that long codes are used for spreading, and that the spreading sequences are orthogonal to each other during symbol interval and are normalized as $|s_k^{(i)}[mN+l]| = 1/\sqrt{N}$.

The kth user spread waveform from transmit antenna i can be written as:

$$\chi_k^{(i)}(t) = \sum_{n=-\infty}^{\infty} u_k^{(i)}[n] \Psi(t - T_c n) \tag{2.35}$$

where $n = mN + l$ is the chip index, t is time index, and $\Psi(t)$ is the normalized Nyquist chip waveform.

The spread signal for the pilot signal for transmit antenna i is:

$$\bar{u}^{(i)}[mN+l] = \bar{A}_i \bar{b}^{(i)}[m] \bar{s}^{(i)}[mN+l] \tag{2.36}$$

where $\bar{A}_i$ is the amplitude of the pilot, $\bar{b}^{(i)}[m]$ is the pilot symbol, and $\bar{s}^{(i)}[mN+l]$ is the pilot spreading sequence for transmit antenna i.

The spread waveform for the pilot symbol for transmit antenna i is:

$$\bar{\chi}^{(i)}(t) = \sum_{n=-\infty}^{\infty} \bar{u}^{(i)}[n]\Psi(t - T_c n). \tag{2.37}$$

From (2.35) and (2.37), the total transmitted signal from transmit antenna i of the base station becomes:

$$\chi^{(i)}(t) = \bar{\chi}^{(i)}(t) + \sum_{k=1}^{K} \chi_k^{(i)}(t). \tag{2.38}$$

The total transmitted signals from each transmit antenna of the base station propagate through time-variant frequency selective fading (multipath) channels.

Let us recall the multipath channels in (2.1).

$$h_{ji}(t) = \sum_{p=0}^{P-1} \alpha_{ji,p}(t) e^{\jmath\theta_{ji,p}(t)} \delta(t - \tau_{ji,p}(t)).$$

Thus, the received signal at the jth receive antenna can be written as:

$$Y^{(j)}(t) \;=\; \sum_{i=1}^{I} \sum_{p=0}^{P-1} \alpha_{ji,p}(t) e^{\jmath\theta_{ji,p}(t)} \chi^{(i)}(t - \tau_{ji,p}(t)) + \mathrm{N}^{(j)}(t), \quad j = 1, 2, \ldots, J \tag{2.39}$$

where $\mathrm{N}^{(j)}$ is the additive white Gaussian noise (AWGN) of the jth receive antenna with mean zero and single sided spectral density σ_n^2.

Note that propagation delay $\tau_{ji,p}(t) = pT_c$ is assumed for simplicity. In addition, if the number of channel multipath $P = 1$, we do not need the equalization. Therefore, we always assume that $P \geq 2$.

At the mobile station, the received signal $Y^{(j)}(t)$ is sampled. Let $r^{(j)}[n]$ denote the nth sampled signal at the chip rate from the output of the matched filter of the jth receive antenna. That is,

$$r^{(j)}[n] = \int_{-\infty}^{\infty} \Psi(\tau) Y^{(j)}(t - \tau) d\tau|_{t = nT_c}. \tag{2.40}$$

Note that from (2.39), we can write the complex attenuation channel as $h^*_{ji}(p;t) = \alpha_{ji,p}(t)e^{\jmath\theta_{ji,p}(t)}$. We assume that the complex attenuation factor of the pth path from transmit antenna i to receive antenna j, $h^*_{ji}[p;n]$ is constant over the chip period, that is,

$$h^*_{ji}[p;n] = \alpha_{ji,p}(t)e^{\jmath\theta_{ji,p}(t)}, \quad nT_c \leq t < (n+1)T_c. \tag{2.41}$$

Then, from (2.40) and (2.41), we can write:

$$r^{(j)}[n] = \sum_{i=1}^{I}\sum_{p=0}^{P-1} h^*_{ji}[p;n]u^{(i)}[n-p] + \eta^{(j)}[n] \tag{2.42}$$

where

$$u^{(i)}[n] = \sum_{k=1}^{K} u^{(i)}_k[n] + \bar{u}^{(i)}[n] \tag{2.43}$$

$$\eta^{(j)}[n] = \int_{-\infty}^{\infty} \Psi(\tau)\mathrm{N}^{(j)}(nT_c - \tau)d\tau. \tag{2.44}$$

Note that $\eta^{(j)}[n]$ is the additive white Gaussian random noise sequence of the jth receive antenna with mean zero and variance σ_n^2.

If the complex channel attenuation is assumed time-invariant for all paths, i.e. $h_{ji}[p;n] = h_{ji}[p]$ for all p, then (2.42) can be written as:

$$r^{(j)}[n] = \sum_{i=1}^{I}\sum_{p=0}^{P-1} h^*_{ji}[p]u^{(i)}[n-p] + \eta^{(j)}[n]. \tag{2.45}$$

Let $\mathbf{h}_{ji}$ be the sampled channel response vector from transmitter i to receiver j of size $P \times 1$. It can be written as:

$$\mathbf{h}_{ji} = (h_{ji}[0] \;\; h_{ji}[1] \;\; \ldots \;\; h_{ji}[P-1])^T. \tag{2.46}$$

We can assemble the $\mathbf{h}_{ji}$ vectors into I separate matrices of size $P \times J$ as follows:

$$\mathbf{H}_i = [\mathbf{h}_{1i} \;\; \mathbf{h}_{2i} \;\; \ldots \;\; \mathbf{h}_{Ji}], \quad i = 1, 2, \ldots, I. \tag{2.47}$$

Furthermore,

$$\mathbf{r}[n] = (r^{(1)}[n] \;\; \ldots \;\; r^{(J)}[n])^T \tag{2.48}$$

$$\mathbf{u}^{(i)}[n] = (u^{(i)}[n] \;\; \ldots \;\; u^{(i)}[n-P+1])^T \tag{2.49}$$

$$\mathbf{n}[n] = (\eta^{(1)}[n] \;\; \ldots \;\; \eta^{(J)}[n])^T \tag{2.50}$$

where $r^{(j)}[n]$ is the received signal at receive antenna j and $u^{(i)}[n]$ is the baseband transmission signal from transmit antenna i. The $J \times 1$ received signal vector $\mathbf{r}[n]$ for the downlink signal model for multiple antennas can be written as:

$$\mathbf{r}[n] = \sum_{i=1}^{I} \mathbf{H}_i^H \mathbf{u}^{(i)}[n] + \mathbf{n}[n]. \tag{2.51}$$

2.6 Existing Receivers for a DS-CDMA System

2.6.1 The Rake Receiver

The rake receiver is the most popular and conventional receiver in the DS-CDMA system [7]. It is called the rake receiver since the receiver has the structure of a rake. The rake receiver based on a single receive antenna is shown in Fig. 2.7.

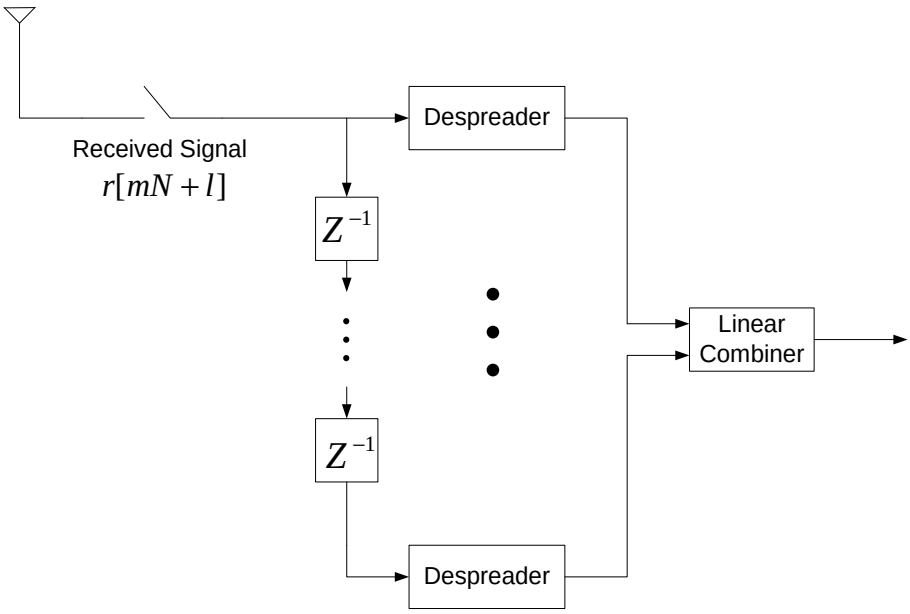

Figure 2.7: The rake receiver

The rake receiver contains a bank of despreaders. Each despreader despreads the received chip sequence according to the desired user. The resulting outputs are combined using a

linear combiner. In order to achieve maximum signal to noise ratio (SNR), the maximal ratio combining (MRC) scheme is used in the linear combiner [38].

Consider the single transmit antenna and single receive antenna case, i.e. $I = J = 1$. The signal model in Section 2.5 becomes:

$$r[mN + l] = r^{(1)}[mN + l] \tag{2.52}$$

$$u[mN + l] = u^{(1)}[mN + l] \tag{2.53}$$

$$h[mN + l] = h_{ji}[mN + l] \tag{2.54}$$

$$\eta[mN + l] = \eta^{(1)}[mN + l] \tag{2.55}$$

where $r[mN + l]$ is the received signal, $u[mN + l]$ is the total transmitted spread signal from the base station, $h[mN + l]$ is the time-variant discrete channel impulse response, and $\eta[mN+l]$ is the additive white Gaussian random noise sequence with mean zero and variance σ_n^2.

From (2.42), we can write:

$$r[mN + l] = \sum_{p=0}^{P-1} h^*[p; mN + l]u[mN + l - p] + \eta[mN + l]. \tag{2.56}$$

From Fig. 2.7, the received signal is delayed and despread in the rake receiver. Assume that user k is the desired user, then the pth despread signal $d_p[m]$ can be written as:

$$d_p[m] = \sum_{m=0}^{N-1} r[mN + l + p]s_k^*[mN + l], \qquad p = 0, \ldots, P - 1 \tag{2.57}$$

where $s_k[mN + l]$ is the long spreading sequence for desired user k.

Assume that $h[p; m]$ is the pth time-variant path of the channel and $\hat{h}[p; m]$ is the channel estimate of $h[p; m]$. The output of the rake receiver at the pth finger becomes:

$$\hat{b}_{RAKE,p}[m] = d_p[m]\hat{h}[p; m]. \tag{2.58}$$

The channel coefficient $h[p;m]$ for $p = 1, \ldots, P$ can be estimated using the pilot signal. The instantaneous channel estimate for the pth path is:

$$\hat{h}[p;m] = \left(\sum_{m=0}^{N-1} r[mN + l + p] \bar{s}^*[mN + l] \right) \bar{b}^*[m] \tag{2.59}$$

where $\bar{s}[mN + l]$ and $\bar{b}[m]$ are the long spreading sequence for the pilot symbol and the pilot signal, respectively.

The instantaneous channel estimate in (2.59) can be smoothed with zero lag for better estimate as:

$$\bar{\hat{h}}[p;m] = \frac{1}{B} \sum_{q=0}^{B-1} \hat{h}[p;m-q] \tag{2.60}$$

where B is the size of moving window.

Under the MRC principle, the decision variables can be obtained by summing up all the combined signals along p as:

$$\hat{b}_{RAKE}[m] = \sum_{p=0}^{P-1} \hat{b}_{RAKE,p}[m]. \tag{2.61}$$

Note that the rake receiver exploits the path diversity and since P despreaders are used, the diversity order P is expected.

There exists a number of modifications of the conventional rake receiver. The linear minimum mean square error criterion was combined with the conventional rake receiver in order to improve the performance [39]. There also exists the space time rake receiver, that is the extension of the rake receiver for multiple receive antennas. It consists of a set of banks of despreaders for the desired user (one bank at each receive antennas), followed by the space time combiner. Several space time rake schemes, including a low complexity space time rake, have been proposed [40]. The only requirement for the rake receiver is that the receiver must know the spreading waveform of the desired user.

2.6.2 The Chip Level Linear Equalizer for CDMA Downlink Channel

The chip level linear equalizer (LE) is a promising approach for CDMA downlink channel receiver. The key idea of using the chip level LE followed by a despreader is to equalize the nonideal downlink channel at the mobile receiver, thus to restore approximately the orthogonality. When the orthogonality is restored, a simple despreader is able to suppress all MAI.

A necessary condition for the receiver to work properly is that the number of users must be smaller than the length of processing gain. In other words, each user is assigned with specific orthogonal spreading codes. The chip level LE directly operates on the received sequence or the different received sequences in order to generate an estimate of the desired user's data symbol sequence. Fig. 2.8 shows the adaptive chip level LE for a single antenna.

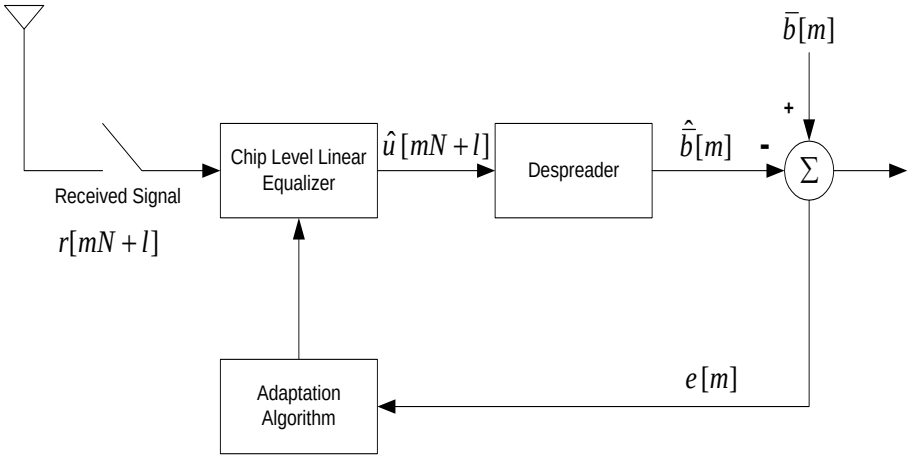

Figure 2.8: The adaptive chip level LE for single antenna

There are two kinds of criterion for the chip level LE: zero forcing (ZF) and MMSE. With the ZF criterion, MAI introduced by multipath can be completely eliminated by full inversion of the downlink channel. However, noise may also be enhanced. The MMSE equalization can be used to minimize the noise enhancement associated with the ZF equalization. In the MMSE equalization, the chip level equalizer measures the error after despreading, and updates the equalizer coefficients at the symbol rate, as shown in Fig. 2.8.

The idea of the linear chip level equalization at the downlink channel for the purpose of restoring the orthogonality of the user spreading sequences was first proposed by Klein [41]. The linear chip level equalization of the downlink for a DS-CDMA system based on the MMSE and ZF criteria was first independently introduced by Frank [12] and Ghauri [42], respectively. The linear chip level equalization of the downlink channel has subsequently been proposed in numerous works [13, 14, 43–46]. An adaptive algorithm that does not require the pilot training sequence has also been proposed [44].

The linear chip level equalization [13] is suitable in the DS-CDMA downlink channel. However, adaptive implementations of the chip level LE are not straightforward, since no continuous multiple user training chip sequence is available. The presence of a continuous pilot signal incorporated in the third generation cellular communication systems has motivated the linear chip level equalization using the continuous pilot channel [5, 14, 46].

Let us consider the linear chip level equalization using the continuous pilot channel for the single transmit antenna and single receive antenna case, i.e. $I = J = 1$. Let us recall (2.52) - (2.55). Then, from (2.45), the received signal can be written as:

$$r[n] = \sum_{p=0}^{P-1} h[p]u[n-p] + \eta[n] \tag{2.62}$$

where $\{h[p]\}$ is the discrete channel impulse response.

Let N_f, $\mathbf{r}[n]$ and $\mathbf{w}$ be the finite length of equalizer, the received signal vector and equalizer vector, respectively.

$$\mathbf{r}[n] = (r[n] \;\; r[n-1] \ldots r[n-N_f+1])^T \tag{2.63}$$

$$\mathbf{w} = (w[0] \;\; w[1] \ldots w[N_f-1])^T. \tag{2.64}$$

The estimate of the transmitted signal can be given by the complex inner product:

$$\hat{u}[n] = \mathbf{w}^H \mathbf{r}[n]. \tag{2.65}$$

The weight vector $\mathbf{w}$ is chosen to minimize the MSE:

$$MSE = E\Big(|\bar{b}[m] - \sum_{m=0}^{N-1} \hat{u}[mN+l+D]\bar{s}^*[mN+l]|^2\Big) \tag{2.66}$$

where D is the delay and $\bar{b}[m]$ is the continuous pilot signal.

In the latest development, Leus *et al.* developed the generalized pilot-based method, called the space time chip level LE for multiple antennas [32, 33]. Their methods are based on the training symbol and semiblind space time chip level LE receivers. Their simulation results show improvements over a pilot-based rake receiver.

2.7 Conclusion

In this chapter, the principle of DS-CDMA system and the general signal model for CDMA MIMO downlink channel are presented. The existing receiver structures for CDMA downlink channel are discussed. We review two receiver structures that can mitigate MAI, and three adaptation algorithms that can track the variation of channel in the time selective fading channel.

Chapter 3

The Chip Level DFE with Multiple Antennas

When the downlink channel of a MIMO CDMA system uses orthogonal spreading codes, frequency selective fading destroys the orthogonality and introduces MAI. Chip level DFE is an attractive method to restore the orthogonality and suppress MAI. Chip level DFE also exploits the benefit of additional diversity gain in the CDMA MIMO downlink channel. Furthermore, Chip level DFE is less affected by the spectral characteristic of the channel. Therefore, it can be expected that the chip level DFE with multiple antennas can improve the performance.

This chapter investigates the performance of chip level DFE for CDMA downlink channel. Two different schemes that are employed at the transmitter, i.e. the space time spreading (STS) scheme and the Alamouti transmit diversity scheme, are investigated.

3.1 The Chip Level DFE with the STS Scheme

This section investigates the performance of chip level DFE for CDMA downlink channel when the STS scheme is employed at the transmitter. In the STS scheme, a set of different

orthogonal codes is assigned to multiple transmit antennas for each user. In principle, any number of transmit antennas can be employed as long as we have a sufficient number of distinct orthogonal codes. In order to estimate channels, the pilot signals are utilized. It is assumed that each antenna continuously transmits its pilot signal (i.e., code-multiplexed pilot is assumed).

3.1.1 Signal Model for DS-CDMA Based on the STS Scheme

Let us consider the previous signal model for DS-CDMA system in Section 2.5. The base station employs user specific orthogonal Walsh-Hadamard spreading codes and a site specific base spreading codes. We assume perfect carrier recovery at the receiver site and there are K users in a CDMA downlink channel.

Let us also consider I transmit antennas and J receive antennas. Each transmit antenna transmits different pilot signals using different orthogonal spreading sequences. Each user is assigned with a different orthogonal spreading codes for each transmit antenna. The block diagram for the transmitter with the STS scheme is shown in Fig. 3.1.

From Fig. 3.1, for $i = 1, 2, \ldots, I$ and $k = 1, 2, \ldots, K$, we can write:

$$b_k[m] = b_k^{(i)}[m] \tag{3.1}$$

$$\bar{A}\bar{b}[m] = \bar{A}_i \bar{b}^{(i)}[m] \tag{3.2}$$

where $b_k[m]$ is the data symbol for the kth user, $\bar{A}$ is the amplitude of the pilot signals, and $\bar{b}[m]$ is the pilot symbol.

Let $u^{(i)}[n]$ be the total baseband transmission signal, transmitted from antenna i at the base station. The received signal at the jth receive antenna is written as:

$$r^{(j)}[n] = \sum_{i=1}^{I} \sum_{p=0}^{P-1} h_{ji}^{*}[p] u^{(i)}[n-p] + \eta^{(j)}[n] \tag{3.3}$$

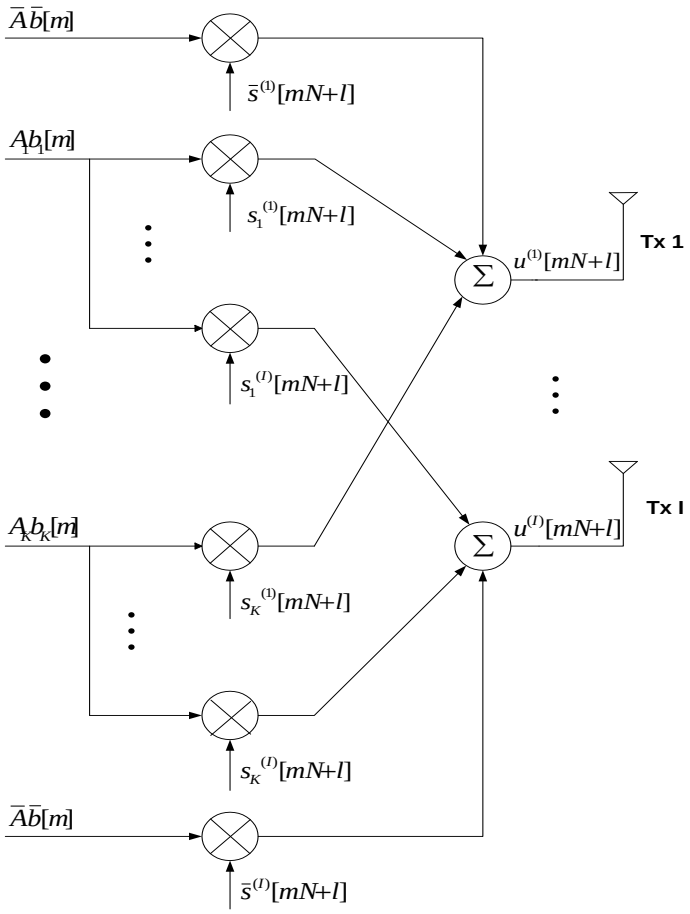

Figure 3.1: Block diagram for the transmitter with the STS scheme using I transmit antennas

where

$$u^{(i)}[mN+l] = \sum_{k=1}^{K} u_k^{(i)}[mN+l] + \bar{u}^{(i)}[mN+l] \tag{3.4}$$

$$u_k^{(i)}[mN+l] = A_k b_k[m] s_k^{(i)}[mN+l] \tag{3.5}$$

$$\bar{u}^{(i)}[mN+l] = \bar{A}\bar{b}[m]\bar{s}^{(i)}[mN+l]. \tag{3.6}$$

In the vector notation, the $J \times 1$ received signal vector can be written as:

$$\mathbf{r}[n] = \sum_{i=1}^{I} \mathbf{H}_i^H \mathbf{u}^{(i)}[n] + \mathbf{n}[n] \tag{3.7}$$

where the channel matrix $\mathbf{H}_i$, the received signal vector $\mathbf{r}[n]$, the transmitted signal vector $\mathbf{u}^{(i)}[n]$, and the noise vector $\mathbf{n}[n]$ are given in (2.47) - (2.50).

3.1.2 The Receiver Structure of the Chip Level DFE with the STS Scheme

In this section, we propose the chip level DFE based on the STS scheme. The block diagram of the scheme is shown in Fig. 3.2. We assume that the decision delays are the same for every data stream, i.e., $D_i = D$ for $i = 1, \ldots, I$. The chip level DFE consists of a feedforward filters $\mathbf{c}_{ij}$ with a temporal span of N_f taps and a feedback filters $\mathbf{g}_{ii}$ with a temporal span of N_b taps.

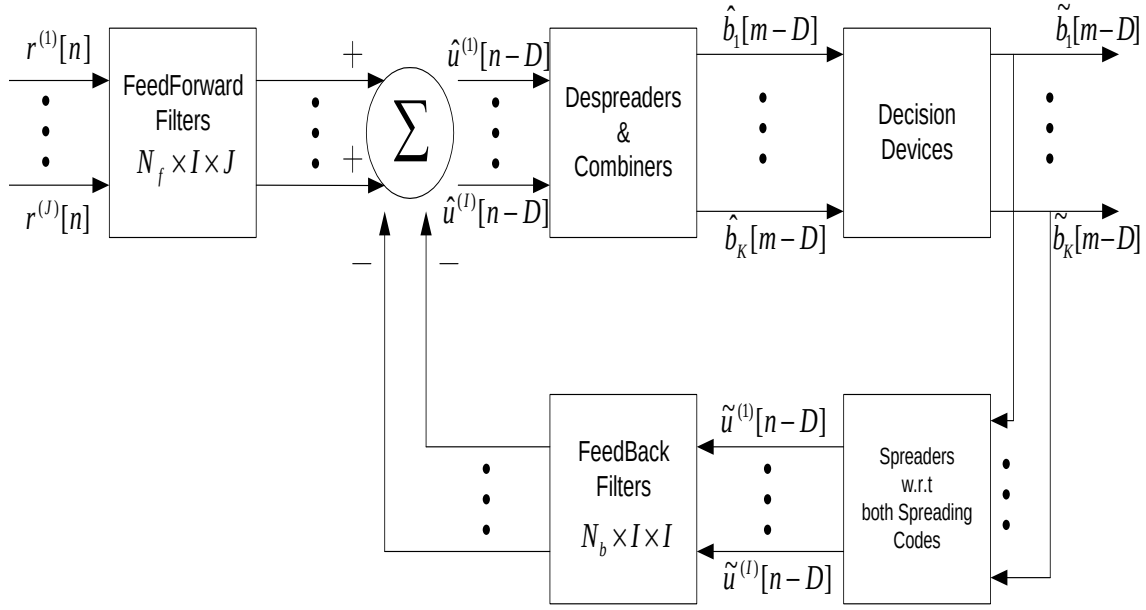

Figure 3.2: The chip level DFE based on the STS architecture with J receive antennas

It is shown in Fig. 3.2 that the chip level DFE is a fully connected receiver, in that past decisions on all data streams are fed back into the detection process for each stream. As a result, it has lower complexity and smaller error propagation than the successive interference cancellation scheme [31].

Although the structure of the forward filter of the chip level DFE appears similar to that of the rake receiver, the operations are different. The rake receiver is to combine the energies of the desired user received through the multipath channel without taking into account the presence of interferers. On the other hand, the forward filter of the chip level DFE works on maximizing the desired user's energy and minimizing the effects of existing interference in

the channel using the MMSE criterion.

The structure of the feedback filter of the chip level DFE is different from the conventional DFE. For the conventional DFE, which is shown in Fig. 2.3, the input signal to the feedback filter is a nonspread (symbol) signal. For the chip level DFE, the input signal to the feedback filter is spread (chip) signal.

The objective of the chip level DFE is to estimate the chip rate sequence $\hat{u}^{(i)}[n], i = 1, \ldots, I$, from which the desired symbol sequence $b_k[m]$ is recovered by despreading the estimated chip rate sequence using the desired user's spreading sequence, as shown in Fig. 3.2.

Let us assume that previous decisions are correct, i.e., $\tilde{u}^{(i)}[n-D] = u^{(i)}[n-D]$ for all i and n.

Let $\mathbf{c}_i$ be the feedforward filters of the ith stream with dimensionality $(N_f J) \times 1$, $\mathbf{g}_i$ be the feedback filters of the ith stream with dimensionality $(N_b I) \times 1$, $\mathbf{\Omega}[n]$ be the N_f J-dimensional symbols spanned by each of the i components of the feedforward filter, and $\mathbf{u}[n-D-1]$ be the correct previous decisions vector with dimensionality $(N_b I) \times 1$. They can be written as:

$$\mathbf{c}_i = (c_{i1}[0] \ \ldots \ c_{iJ}[0] \ \ldots \ c_{i1}[N_f-1] \ \ldots \ c_{iJ}[N_f-1])^T \quad (3.8)$$

$$\mathbf{g}_i = (g_{i1}[1] \ \ldots \ g_{i1}[N_b] \ \ldots \ g_{iI}[1] \ \ldots \ g_{iI}[N_b])^T \quad (3.9)$$

$$\mathbf{\Omega}[n] = (\mathbf{r}^T[n] \ \mathbf{r}^T[n-1] \ \ldots \ \mathbf{r}^T[n-N_f+1])^T \quad (3.10)$$

$$\mathbf{u}[n-D-1] = \begin{pmatrix} u^{(1)}[n-D-1] \\ \vdots \\ u^{(1)}[n-D-N_b] \\ \vdots \\ u^{(I)}[n-D-1] \\ \vdots \\ u^{(I)}[n-D-N_b] \end{pmatrix}. \quad (3.11)$$

The total output of the chip level DFE is:

$$\hat{u}^{(i)}[n-D] = \mathbf{w}_i^H \mathbf{d}[n] \quad (3.12)$$

where $\mathbf{w}_i$ and $\mathbf{d}[n]$ are the complete equalizer vector and complete data vector, respectively, and they can be written as:

$$\mathbf{w}_i = (\mathbf{c}_i^T \quad \mathbf{g}_i^T)^T \tag{3.13}$$

$$\mathbf{d}[n] = (\mathbf{\Omega}^T[n] \quad -\mathbf{u}^T[n-D-1])^T. \tag{3.14}$$

Let us denote:

$$\mathbf{z}_i[m] = \sum_{l=0}^{N-1} \mathbf{d}[mN+l+D]\bar{s}^{*(i)}[mN+l]. \tag{3.15}$$

Then, the MSE function of the chip level DFE-despreader can be written as:

$$MSE_i = E\Big(|\bar{b}[m] - \mathbf{w}_i^H \mathbf{z}_i[m]|^2\Big), \qquad i = 1, 2, \ldots, I. \tag{3.16}$$

3.2 The Chip Level DFE with the Alamouti Scheme

While chip level DFE with STS scheme presented in Section 3.1 offers diversity gain and simplicity in the demodulation, it requires additional spreading codes for each user in each transmit antenna. With I transmit antennas, I times more codes are needed, and with a limited number of orthogonal codes, this also means that I times fewer users can simultaneously be supported. This leads to the STTD scheme that has been proposed by Alamouti with two transmit antennas [27]. The Alamouti scheme is simple to implement and has been employed in a third generation system [47]. The Alamouti scheme does not require different spreading codes for each transmit antennas. As a result, more spreading codes are available to support more users than the STS scheme.

In this section, we consider the chip level DFE when the Alamouti scheme is employed at the transmitter for downlink transmission. It is assumed that each antenna continuously transmits its pilot signal and channels are estimated by using the code multiplexed pilot.

3.2.1 Signal Model for DS-CDMA Based on the Alamouti Scheme

Consider the discrete time complex baseband model for the downlink channel of a single cell direct sequence CDMA system. As before, there are K users in the system and the base station employs long spreading codes. We consider the Alamouti transmit diversity scheme with two transmit antennas [27]. Fig. 3.3 shows the diagram.

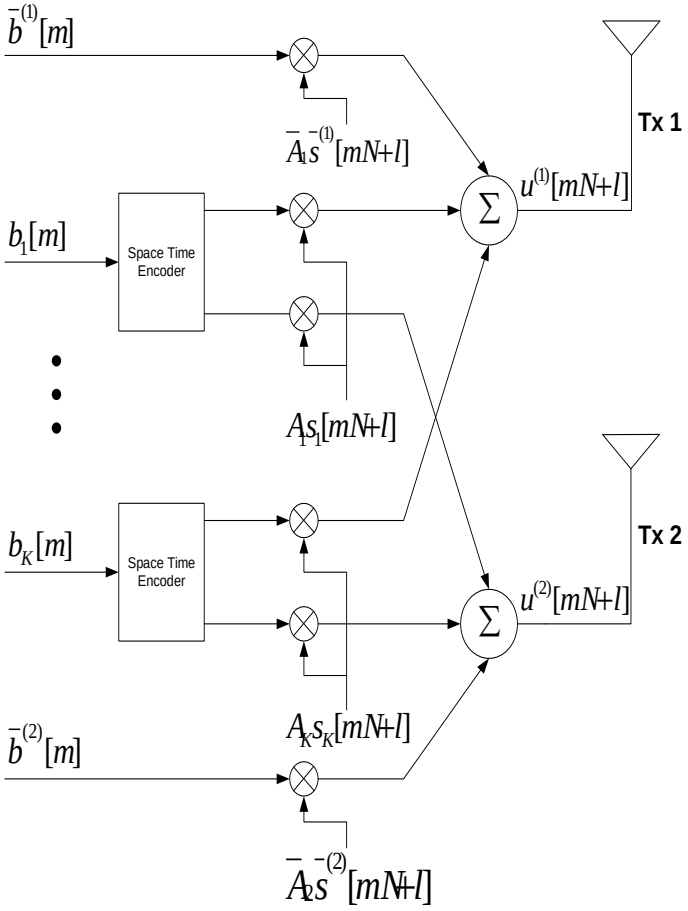

Figure 3.3: Block diagram for the transmitter with the Alamouti scheme

Let $b_k[m]$ be the mth symbol of transmission to mobile station k and independent and identical distributed (i.i.d.). We also assume that quadrature phase shift keying (QPSK) signalling is used. That is, $b_k[m] \in \{\pm 1 \pm j\}$. Then, the outputs of the space time encoder [27] become:

$$\begin{aligned} b_k^{(1)}[2m] &= b_k[2m] \\ b_k^{(1)}[2m+1] &= -b_k^*[2m+1] \end{aligned}$$

$$
\begin{aligned}
b_k^{(2)}[2m] &= b_k[2m+1] \\
b_k^{(2)}[2m+1] &= b_k^*[2m]
\end{aligned}
$$

where $b_k^{(i)}[m]$ is the data symbol from transmit antenna i to the kth user.

From Fig. 3.3, we can also see that the same user spreading sequence is used for the data symbol $b_k^{(i)}[m]$. That is,

$$
s_k[mN+l] = s_k^{(i)}[mN+l] \qquad i = 1, 2 \tag{3.17}
$$

where $s_k[mN+l]$ is the kth user long spreading sequence.

We also assumed that the long spreading sequence is normalized as $|s_k[mN+l]| = \frac{1}{\sqrt{N}}$.

For coherent combining and channel estimation at the receiver, as shown in Fig. 3.3, two different orthogonal pilot spreading sequences ($\bar{s}^{(i)}[n], i = 1, 2$) with different pilot symbols ($\bar{b}^{(i)}[m], i = 1, 2$) can be transmitted through two transmit antennas.

Assume that the complex channel attenuations associated with each pair of transmit and receive antennas are time-invariant. Then, the received signal at the jth receive antenna can be written as:

$$
r^{(j)}[mN+l] = \sum_{i=1}^{2} \sum_{p=0}^{P-1} h_{ji}^*[p] u^{(i)}[mN+l-p] + \eta^{(j)}[mN+l] \tag{3.18}
$$

where

$$
\begin{aligned}
u^{(i)}[mN+l] &= \sum_{k=1}^{K} u_k^{(i)}[mN+l] + \bar{u}^{(i)}[mN+l] && (3.19) \\
u_k^{(i)}[mN+l] &= A_k b_k^{(i)}[m] s_k[mN+l] && (3.20) \\
\bar{u}^{(i)}[mN+l] &= \bar{A}_i \bar{b}^{(i)}[m] \bar{s}^{(i)}[mN+l]. && (3.21)
\end{aligned}
$$

In the vector notation, $J \times 1$ received signal vector can be written as:

$$
\mathbf{r}[n] = \sum_{i=1}^{2} \mathbf{H}_i^H \mathbf{u}^{(i)}[n] + \mathbf{n}[n] \tag{3.22}
$$

where the channel matrix $\mathbf{H}_i$, the received signal vector $\mathbf{r}[n]$, the transmitted signal vector $\mathbf{u}^{(i)}[n]$, and the noise vector $\mathbf{n}[n]$ are given in (2.47) - (2.50).

3.2.2 The Receiver Structure of the Chip Level DFE with the Alamouti Scheme

In this section, we propose the chip level DFE for the Alamouti transmit diversity scheme, as shown in Fig. 3.4. As in previous section, we assume that the decision delays are the same for every data stream, i.e., $D_i = D$ for $i = 1, 2$.

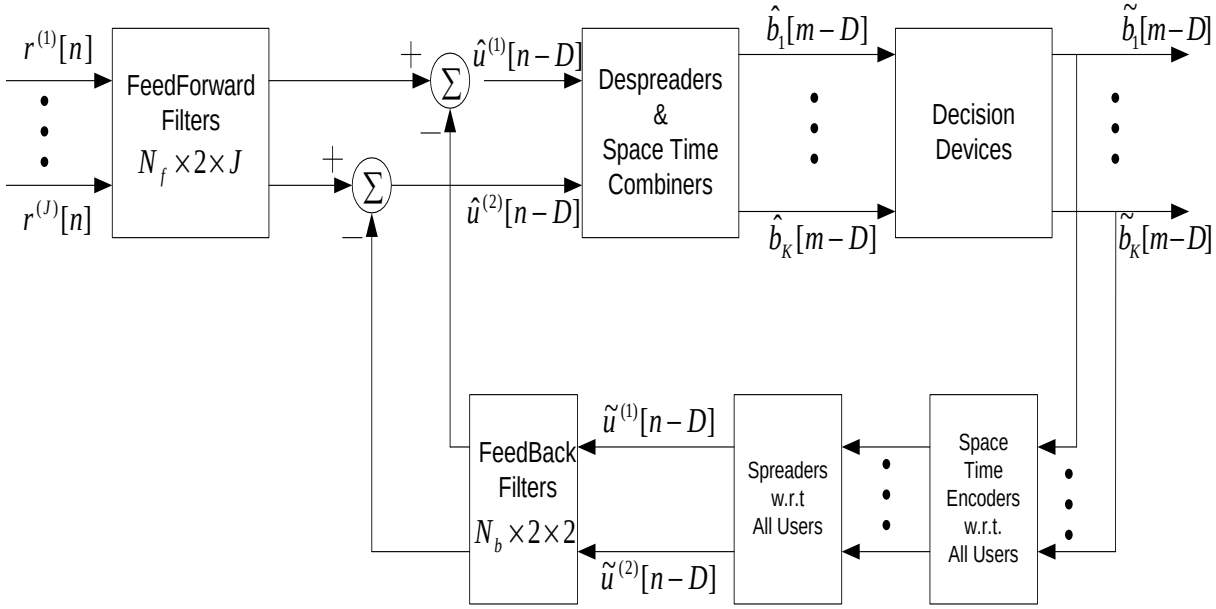

Figure 3.4: The chip level DFE with the Alamouti scheme

The chip level DFE can bring the signals closer to orthogonal. In the feedforward path, the despreaders suppress MAI after the equalization and then the space time combiners are applied to combine the space time encoded signal. In the feedback path, the space time encoder is used to encode the decision symbol, and the spreaders follow to provide the spread (chip) signal to the feedback filter.

The objective of the chip level DFE based on the Alamouti scheme is to estimate the chip rate sequence $\hat{u}^{(i)}[n], i = 1, 2$, from which the desired symbol sequence $b_k[m]$ is recovered by despreading and combining the chip rate sequence, as shown in Fig. 3.4.

Using the same approach as in Section 3.1, the total output of the chip level DFE can be

written as:

$$\hat{u}^{(i)}[n-D] = \mathbf{w}_i^H \mathbf{d}[n] \quad i = 1, 2 \tag{3.23}$$

where $\mathbf{w}_i$ and $\mathbf{d}[n]$ are given in (3.13) and (3.14), with their associated expressions in (3.8)-(3.11).

The equalization vectors, $\mathbf{w}_i$, should be optimized to suppress ICI as well as the interference from the other antennas, as a result of using multiple transmit antennas. If the interfering signal from the other transmit antennas is not suppressed, the chip level equalization followed by despreading cannot be effective to restore the orthogonality of the signal.

Let $\mathbf{\Omega}[n]$ be the N_f J-dimensional symbols spanned by each of the i components of the feedforward filter. That is,

$$\begin{aligned} \mathbf{\Omega}[n] &= (\mathbf{r}^T[n] \;\; \mathbf{r}^T[n-1] \;\; \ldots \;\; \mathbf{r}^T[n-N_f+1])^T & (3.24) \\ &= \sum_{i=1}^{2} \bar{\mathbf{H}}_i^H \bar{\mathbf{u}}^{(i)}[n] + \bar{\mathbf{n}}[n] & (3.25) \end{aligned}$$

where $\bar{\mathbf{u}}^{(i)}[n]$ is the extended sequence of baseband transmission signal vector, $\bar{\mathbf{H}}_i$ is the block Toeplitz channel matrix with $(P + N_f - 1)$ rows and JN_f columns, and $\bar{\mathbf{n}}[n]$ is the extended sequence of noise vector. In detail, they can be written as:

$$\begin{aligned} \bar{\mathbf{u}}^{(i)}[n] &= (u^{(i)}[n] \;\; u^{(i)}[n-1] \ldots \;\; u^{(i)}[n-P-N_f+2])^T & (3.26) \\ \bar{\mathbf{H}}_i &= \begin{pmatrix} \mathbf{H}_i & \ldots & \mathbf{0} \\ \vdots & \ddots & \vdots \\ \mathbf{0} & \ldots & \mathbf{H}_i \end{pmatrix} & (3.27) \\ \bar{\mathbf{n}}[n] &= (\mathbf{n}^T[n] \;\; \mathbf{n}^T[n-1] \ldots \;\; \mathbf{n}^T[n-N_f+1])^T. & (3.28) \end{aligned}$$

From Fig. 3.3, $\bar{b}^{(i)}[m]$ is the pilot symbol for antenna i. Then, the MSE function of the chip level DFE-despreader, which is decided to optimize the equalization vector $\mathbf{w}_i$, can be written as:

$$MSE_i = E\Big(|\bar{b}^{(i)}[m] - \sum_{l=0}^{N-1} \mathbf{w}_i^H \mathbf{d}[mN+l+D]\bar{s}^{*(i)}[mN+l]|^2\Big), \qquad i = 1, 2. \tag{3.29}$$

Thus, the optimum equalizer vector can be found as:

$$\mathbf{w}_i = \frac{E(\sum_{l=0}^{N-1} \mathbf{d}[mN+l+D]\bar{s}^{*(i)}[mN+l]\bar{b}^{*(i)}[m])}{E(\sum_{l=0}^{N-1}\sum_{l'=0}^{N-1}\mathbf{d}[mN+l+D]\bar{s}^{*(i)}[mN+l]\bar{s}^{(i)}[mN+l']\mathbf{d}^H[mN+l'+D])}. \quad (3.30)$$

Assume the following:

A1) All spreading sequences are orthogonal in the symbol duration and

$$\sum_{l=0}^{N-1} s_k[mN+l]s_{k'}^*[mN+l] = \delta_{k,k'}, \quad m=-\infty,\ldots,0,\ldots,\infty, \quad k,k'=1,\ldots,K$$

where δ is the Kronecker delta function.

A2) $s_k[n]$, $s_{k'}[n]$, $k \neq k'$, and $\bar{s}^{(i)}[n]$ have zero mean and are independent of each other, and

$$E(s_k[n]s_k^*[n']) = E(\bar{s}^{(i)}[n]\bar{s}^{*(i)}[n']) = \frac{1}{N}\delta_{n,n'}.$$

A3) $s_k[n]$, $k=1,\ldots,K$ and $\eta[n]$ are independent of each other.

Then, the closed form solution of the optimal equalization vector becomes:

$$\mathbf{w}_i = \begin{pmatrix} \mathbf{c}_i \\ \mathbf{g}_i \end{pmatrix} = \mathbf{R}^{-1}\mathbf{p}_i, \qquad i=1,2 \quad (3.31)$$

where

$$\mathbf{p}_i = \bar{A}\sigma_b^2 \begin{pmatrix} (\bar{\mathbf{H}}_i)_{D+1}^H \\ \mathbf{0} \end{pmatrix} \quad (3.32)$$

$$\mathbf{R} = \beta \begin{pmatrix} \frac{\mathbf{R}_{11}}{\beta} & -(\bar{\mathbf{H}}_1)_{D+2:D+N_b+1}^H & -(\bar{\mathbf{H}}_2)_{D+2:D+N_b+1}^H \\ -(\bar{\mathbf{H}}_1)_{D+2:D+N_b+1} & \mathbf{I} & \mathbf{0} \\ -(\bar{\mathbf{H}}_2)_{D+2:D+N_b+1} & \mathbf{0} & \mathbf{I} \end{pmatrix} \quad (3.33)$$

$$\mathbf{R}_{11} = \beta\sum_{i=1}^{2}\bar{\bar{\mathbf{H}}}_i^H\bar{\bar{\mathbf{H}}}_i + |\bar{A}|^2\sigma_b^2(\bar{\mathbf{H}}_i)_{D+1}^H(\bar{\mathbf{H}}_i)_{D+1} + \sigma_n^2\mathbf{I} \quad (3.34)$$

$$\beta = \frac{P_s+|\bar{A}|^2}{N}\sigma_b^2 \quad (3.35)$$

$$P_s = \sum_{k=1}^{K}|A_k|^2 \quad (3.36)$$

where $\mathbf{I}$ is the identity matrix, $\mathbf{0}$ is the null matrix, $(\cdot)_{D+1}$ indicates the $(D+1)$th row of the corresponding matrix, $(\cdot)_{D+2:D+N_b+1}$ indicates rows $(D+2)$ to $(D+N_b+1)$, P_s is the total transmitted power of users, $\bar{\bar{\mathbf{H}}}_i$ is the matrix which is obtained from $\bar{\mathbf{H}}_i$ with removing the $(D+1)$th row vector, σ_b^2 is the variance of data symbol, σ_n^2 is the noise variance, and $\bar{A} = \bar{A}_i$ is the amplitude of the pilot signal.

Proof: See Appendix B.

In addition, the MMSE is found from (3.31) - (3.34) as:

$$MMSE_i = \sigma_b^2 - \sigma_b^2 \bar{A}^* [(\bar{\mathbf{H}}_i)_{D+1} \;\; \mathbf{0}] \mathbf{w}_i, \qquad i = 1, 2. \tag{3.37}$$

It is interesting to see whether the assumptions **A1**) - **A3**) and the result of the MMSE theoretical analysis in (3.37) hold with practical scrambled Walsh codes. In order to see this, we used Matlab to perform Monte Carlo simulation. Two transmit and two receive antennas are assumed in the system. Let $\mathbf{h}_{ji}[n]$ be the impulse response of the complex channel from transmit antenna i to receive antenna j and suppose the Z-transform of the impulse response of the channels is given by:

$$\begin{aligned}
H_{11}(z) &= 1 + (0.2 + j1.2)z^{-1} + (-0.08 + j0.24)z^{-2} - j0.096z^{-3} \\
H_{12}(z) &= 1 + (1.2 + j0.7)z^{-1} + (-0.06 + j0.84)z^{-2} - 0.072z^{-3} \\
H_{21}(z) &= 1 + (0.1 - j1.4)z^{-1} + (-0.2 - j0.14)z^{-2} + j0.28z^{-3} \\
H_{22}(z) &= 1 - z^{-1} + 0.64z^{-2} - 0.64z^{-3}.
\end{aligned}$$

Let us assume that there are 10 users including the pilot symbol, the processing gain is 16, SNR is 10 dB, the delay D is 3, and the signal amplitudes are the same and normalized (i.e., $A_k = \bar{A} = 1$). In addition, the length of the feedforward filter and the feedback filter are set to 7 and 4, respectively. The simulation results are obtained with 1000 samples (i.e., 1000 symbols) and 50 realizations. The scrambled Walsh codes are used for spreading. The theoretical and simulated MMSE of the chip level DFE from (3.37) are shown to confirm the MMSE analysis in Fig. 3.5 and Fig. 3.6.

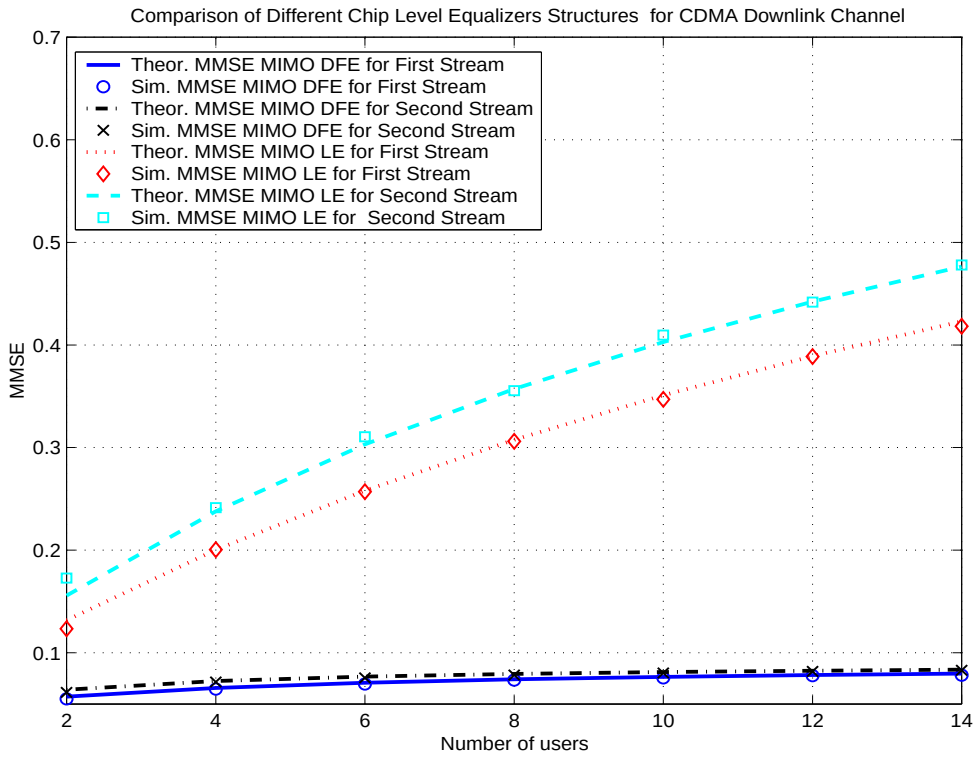

Figure 3.5: Theoretical MMSE and simulation results of the chip level DFE and the chip level LE based on the Alamouti scheme for different numbers of users (lines represent the theoretical results and marks represent the simulation results)

From Fig. 3.5 and Fig. 3.6, we observe that the simulation results are in accordance with the theoretical results, which support the validity of the MMSE approach for the chip level DFE based on the Alamouti scheme. Fig. 3.5 and Fig. 3.6 also show that the chip level DFE outperforms the chip level LE.

The performance of the chip level DFE is less sensitive to the spectral channel characteristic [20]. The chip level DFE can suppress ICI more efficiently compared to the chip level LE. Therefore, in a heavy load system (larger number of users), the chip level DFE offers significant improvement, as shown in Fig. 3.5.

At higher SNR, MAI is more dominant than noise. As a result, at higher SNR, the chip level DFE can suppress MAI more and offer significant improvement, as confirmed by the results shown in Fig. 3.6.

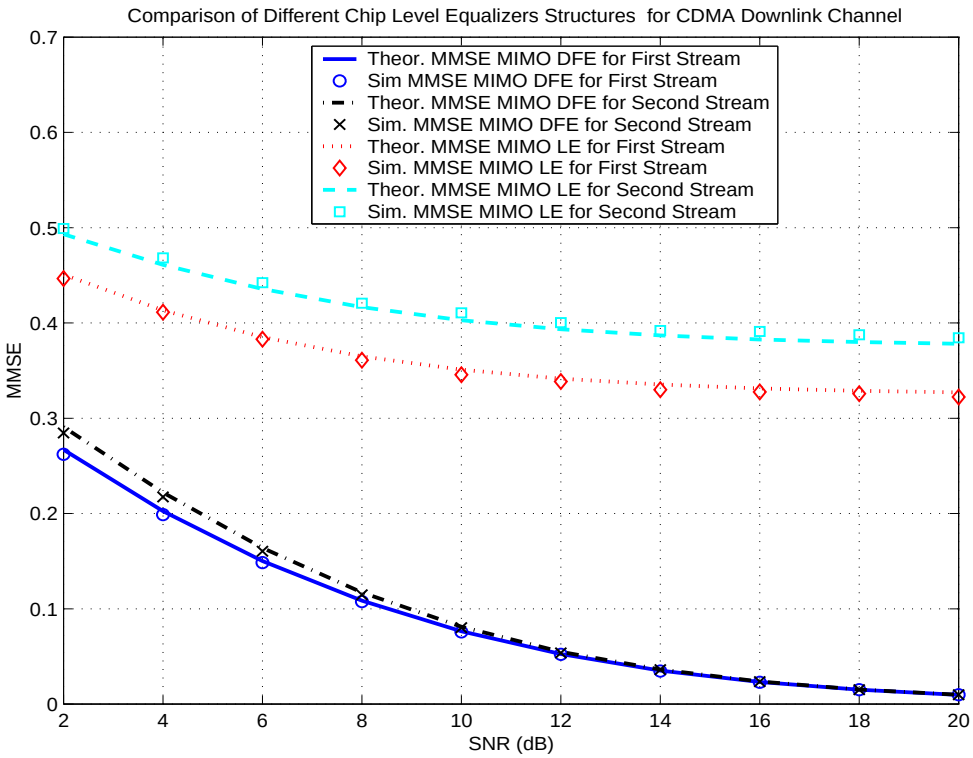

Figure 3.6: Theoretical MMSE and simulation results of the chip level DFE and the chip level LE based on the Alamouti scheme for different SNRs (lines represent the theoretical results and marks represent the simulation results)

3.3 The Adaptive Chip Level DFE

In the third generation wireless system, the continuous pilot signal is available [5] and equalization can be carried out with this continuous pilot signal. Therefore, adaptive equalization can be performed. The equalizers can update their coefficients at the symbol rate and can track the variation of the channel continuously. The adaptation algorithm in the form of the LMS adaptive transversal filter can track the channel variation and thus, can update the equalizer coefficients.

Let us recall (3.16) and (3.29). The MSE function of the chip level DFE-despreader is written as:

$$MSE_i = E\left(|\bar{b}^{(i)}[m] - \mathbf{w}_i^H \mathbf{z}_i[m]|^2\right) \tag{3.38}$$

where $\mathbf{z}_i[m]$ is given in (3.15).

For the LMS algorithm to work, we need to set the initial value of the ith tap-weight vector $\hat{\mathbf{w}}_i[m]$. If prior knowledge on the ith tap-weight vector $\hat{\mathbf{w}}_i[m]$ is available, we can use it to select an appropriate value for $\hat{\mathbf{w}}_i[0]$. Otherwise, we can set $\hat{\mathbf{w}}_i[0] = \mathbf{0}$.

Let us recall Section 2.3. From (3.38), the adaptation of the equalizer coefficients based on the LMS algorithm for $m = 0, 1, 2, \ldots$ can be written as:

$$e^{(i)}[m] = \bar{b}^{(i)}[m] - \hat{\mathbf{w}}_i^H[m]\mathbf{z}_i[m] \tag{3.39}$$

$$\hat{\mathbf{w}}_i[m+1] = \hat{\mathbf{w}}_i[m] + \mu e^{*(i)}[m]\mathbf{z}_i[m] \tag{3.40}$$

where $e^{(i)}[m]$ is the ith a posteriori error signal, $\hat{\mathbf{w}}_i[m]$ and $\hat{\mathbf{w}}_i[m+1]$ are the current value and the updated value of the ith complete equalizer vector, respectively.

From the cost function in (3.38), we can also have the normalized LMS (NLMS) algorithm as follows:

$$\hat{\mathbf{w}}_i[m+1] = \hat{\mathbf{w}}_i[m] + \frac{\bar{\mu}}{\|(\mathbf{z}_i[m])\|^2} e^{*(i)}[m]\mathbf{z}_i[m]. \tag{3.41}$$

Note that the updating has been carried out at the symbol rate and the adaptation gain shall be properly chosen to track the variation of channel.

We can use other adaptive algorithms such as the RLS algorithm to give faster convergence rate. The RLS algorithm requires the initial value of the ith inverse correlation matrix $\mathbf{P}_i[0]$ and the ith equalizer vector $\hat{\mathbf{w}}_i[0]$. That is,

$$\mathbf{P}_i[0] = \varsigma^{-1}\mathbf{I} \tag{3.42}$$

$$\hat{\mathbf{w}}_i[0] = \mathbf{0} \tag{3.43}$$

where ς is the small positive constant.

The RLS algorithm for $m = 1, 2, \ldots$, can be written as:

$$\mathbf{k}_i[m] = \frac{\mathbf{P}_i[m-1]\mathbf{z}_i[m]}{\lambda + \mathbf{z}_i^H[m]\mathbf{P}_i[m-1]\mathbf{z}_i[m]} \tag{3.44}$$

$$\varepsilon^{(i)}[m] = \bar{b}^{(i)}[m] - \hat{\mathbf{w}}_i^H[m-1]\mathbf{z}_i[m] \tag{3.45}$$

$$\hat{\mathbf{w}}_i[m] = \hat{\mathbf{w}}_i[m-1] + \varepsilon^{*(i)}[m]\mathbf{k}_i[m] \tag{3.46}$$

$$\mathbf{P}_i[m] = \frac{\mathbf{P}_i[m-1] - \mathbf{k}_i[m]\mathbf{z}_i^H[m]\mathbf{P}_i[m-1]}{\lambda} \tag{3.47}$$

where $\mathbf{k}_i[m]$ is the ith gain vector, $\varepsilon^{*(i)}[m]$ is the ith a priori error signal, $\hat{\mathbf{w}}_i[m]$ is the ith complete equalizer vector, and $\mathbf{P}_i[m]$ is the ith inverse correlation matrix.

Chapter 4

Simulation Studies

The performance of the rake receiver and the adaptive chip level DFE is investigated and compared under various simulation environments. For the performance comparative study, we consider 4 receivers: the rake receiver for single antenna, the rake receiver for multiple antennas, the chip level DFE for single antenna, and the chip level DFE for multiple antennas.

4.1 Simulation Environment

In this simulation, we used Matlab to perform Monte Carlo simulation. We consider single antenna systems and multiple antennas (MIMO) systems. For the MIMO systems, two transmit and two receive antennas are employed. Time-variant frequency selective fading channels with 4 multipaths using Jakes model are considered. In this model, the autocorrelation is given as [19]:

$$E[h_{ji}(p;n)h^*_{j'i'}(p';n')] = J_0(2\pi f_D T_c|n-n'|)\delta_{p,p'}\delta_{i,i'}\delta_{j,j'} \tag{4.1}$$

where $J_0(\cdot)$ is the zero-order Bessel function of the first kind, f_D is the maximum Doppler frequency, T_C is the chip duration, and δ is the Kronecker delta function. The maximum Doppler frequency is decided by the speed of mobile terminal.

The carrier frequency f_c is assumed to be 2 GHz and the speed of the mobile is set to 60 km/hr. The spreading sequences from the Walsh codes of length 32 with scrambling are used. The data rate is set to 128 kbps and the chip rate is set to 4.096 Mcps.

The transmission powers are assumed to be the same, i.e., $A_k = \bar{A}_i = 1; i = 1, 2$, with a SNR of 10 dB. The number of users K is set to 16. The orthogonal pilot signals in each transmit antenna are continuously transmitted. For signaling, we use uncoded quadrature phase shift keying (QPSK).

The tap numbers in the feedforward filter and the feedback filter for the chip level DFE based on the Alamouti scheme are set to 7 and 4, respectively. The tap numbers in the feedforward and the feedback filters for the chip level DFE based on the STS are set to 5 and 3, respectively. Note that the filter tap numbers have been properly decided to achieve the best performance, and that they depend on the variation of the channel and the SNR. In addition, the correct feedback is assumed for the chip level DFE and the perfect CSI for the rake receiver. For the performance indicator, the BER is used; the average BER over all users has been computed. In order to handle the problems caused by channel variations, we consider the NLMS and the RLS algorithms.

4.2 Simulation Results of the Chip Level DFE with the STS Scheme

The adaptation gain $\bar{\mu}$ for the NLMS algorithm must be properly decided to have the best performance. In this specific simulation environment, the best adaptation gains for the chip level DFE based on single antenna and multiple antennas cases are 0.4 and 0.8, respectively, as shown in Fig. 4.1.

In Fig. 4.2, the BER performance with respect to the number of users using the NLMS adaptation algorithm is shown. As the number of transmissions increases, the performance for all receivers (the rake and the DFE) becomes worse due to increasing MAI. Since the

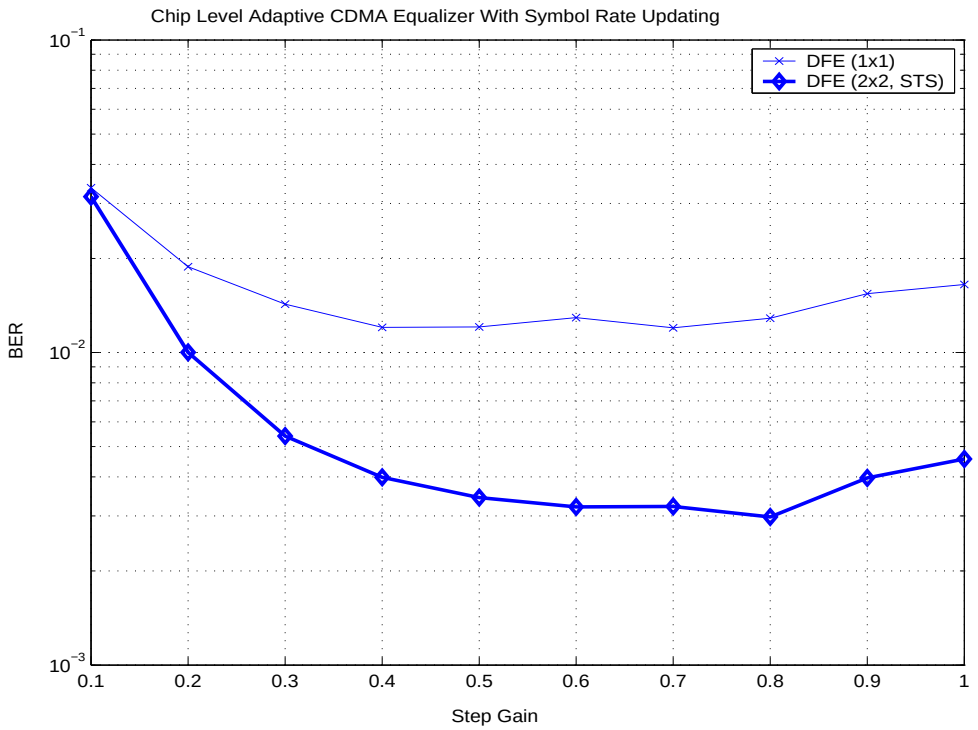

Figure 4.1: BER performance of the chip level DFE based on the STS scheme with respect to the adaptation gain using the NLMS adaptation algorithm

equalization is not perfect under a time-variant fading environment, it is observed that the equalizer is also affected by MAI. However, the chip level DFE generally outperforms the rake receiver. For example, at a BER of 10^{-3}, the chip level DFE can accommodate about one and half times more users than the rake receiver (when multiple antennas are used). It can also be observed from Fig. 4.2 that the significant BER improvement for both the rake receiver and the chip level DFE can be achieved when multiple antennas are used.

The BER results are shown in Fig. 4.3 for various values of SNR using the NLMS adaptation algorithm. At lower SNR, the background noise is dominant and therefore diversity gain is needed to provide better performance. At higher SNR, MAI becomes dominant and the equalization can provide better performance by suppressing MAI. Therefore, the performance of the rake receiver becomes saturated with high SNR. On the other hand, the performance of the chip level DFE is improved for higher SNR. As before, the performance in both receivers is also improved significantly when multiple antennas are used.

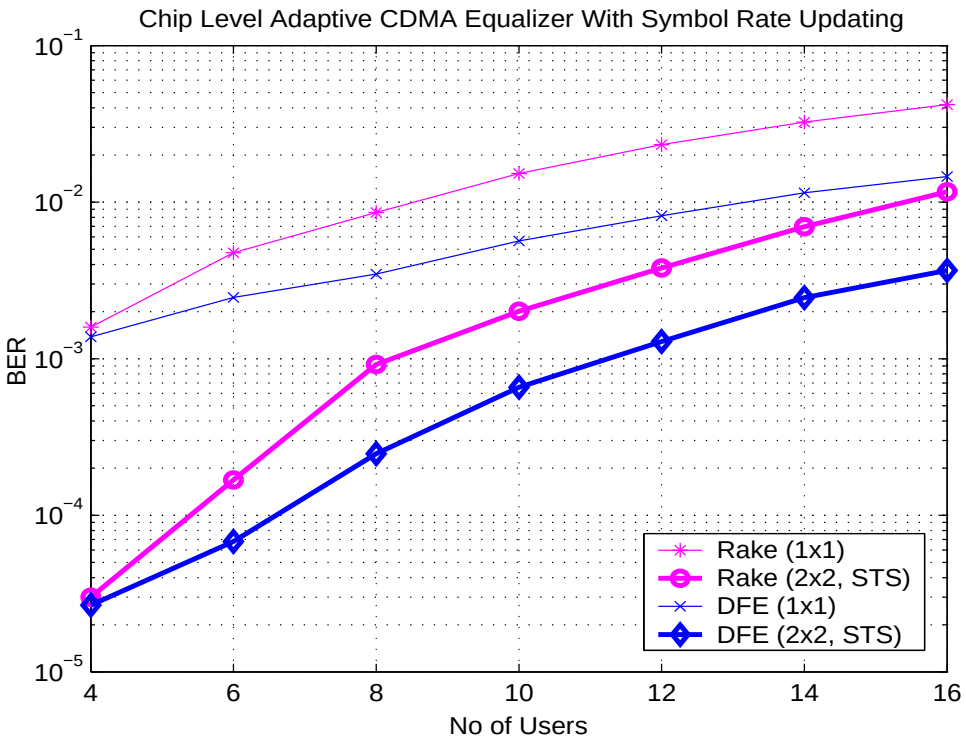

Figure 4.2: BER performance of the chip level DFE based on the STS scheme with respect to the number of users using the NLMS adaptation algorithm

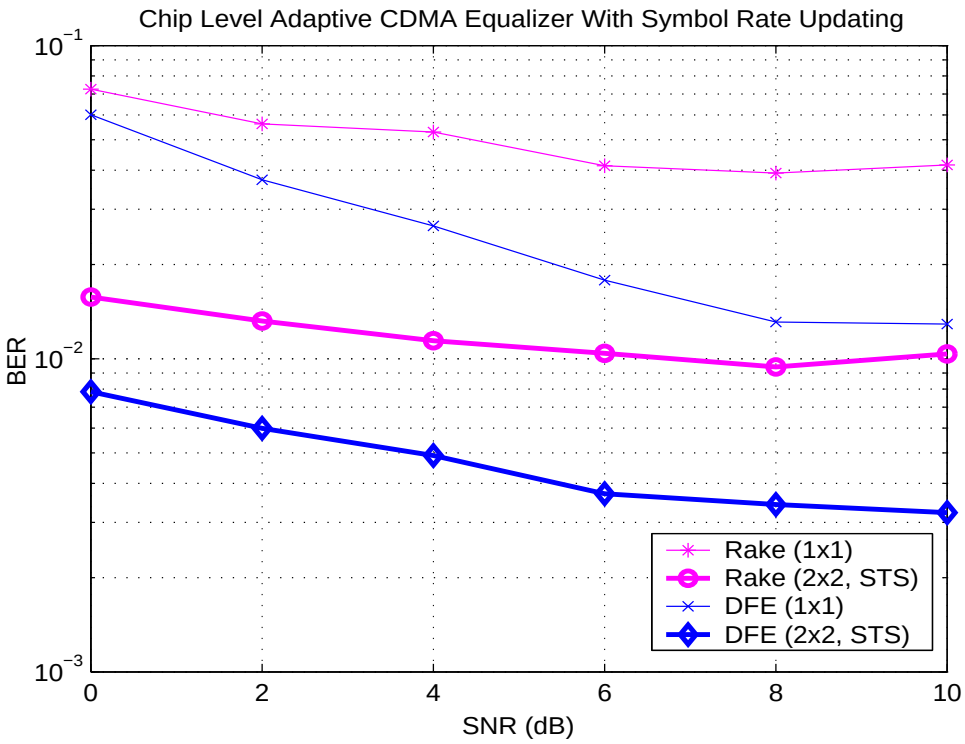

Figure 4.3: BER performance of the chip level DFE based on the STS scheme with respect to SNR using the NLMS adaptation algorithm

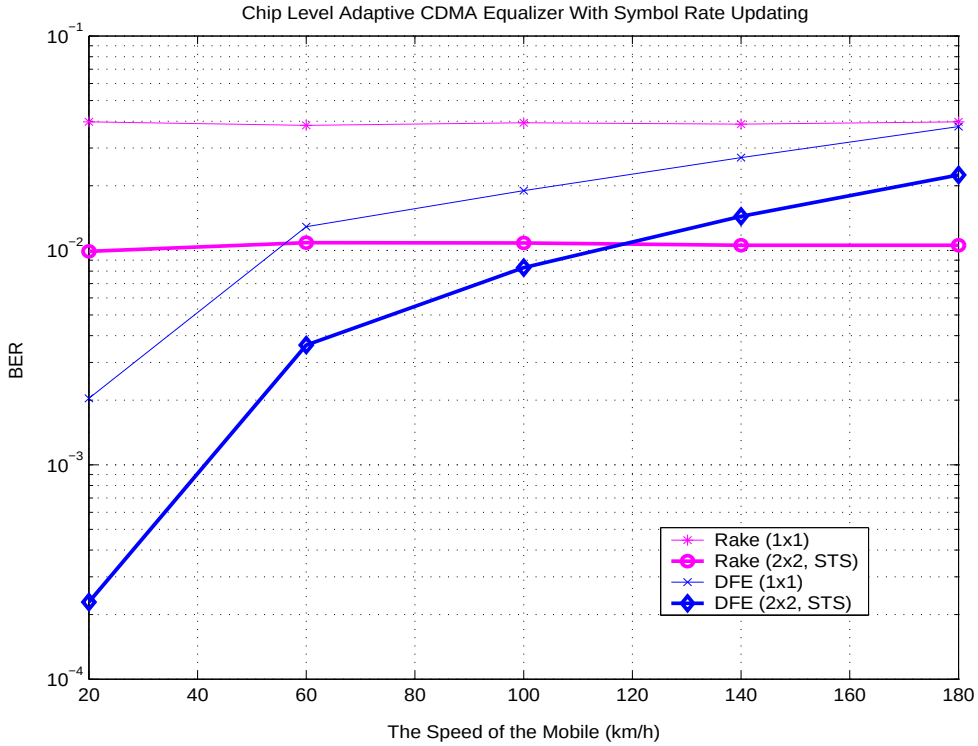

Figure 4.4: BER performance of the chip level DFE based on the STS scheme with respect to the speed of the mobile using the NLMS adaptation algorithm

In general, it is expected that the receiver performance is degraded when the variation of the channel is high. Fig. 4.4 illustrates this phenomena. Note that the variation of the channel does not affect the performance of the rake receiver since the performance degradation is only due to the channel estimation error (we assume perfect CSI for the rake receiver). The performance of the adaptive equalizer deteriorates as the speed of the mobile increases. It is because the adaptive equalizer becomes difficult to cope with the variation of the channel. For example, at a BER of 10^{-2}, the rake receiver outperforms the chip level DFE, when the speed of the mobile is higher than 120 km/hr (when multiple antennas are used). To overcome this problem, some better adaptive algorithms that provide better tracking performance, can be used to improve the BER performance at the expense of increasing computational complexity.

4.3 Simulation Results of the Chip Level DFE with the Alamouti Scheme

The adaptation gain and the forgetting factor for the adaptation algorithm have to be properly decided to achieve the best performance. Fig. 4.5 and Fig. 4.6 show that the best adaptation gain $\bar{\mu}$ and the optimum forgetting factor λ for the chip level DFE based on single transmit and receive antenna are 0.2 and 0.97, respectively. For the chip level DFE based on multiple antennas, the adaptation gain $\bar{\mu}$ of 0.3 and the forgetting factor λ of 0.97 are set. Note that the adaptation gain and the forgetting factor depend on the variation of the channel and the SNR.

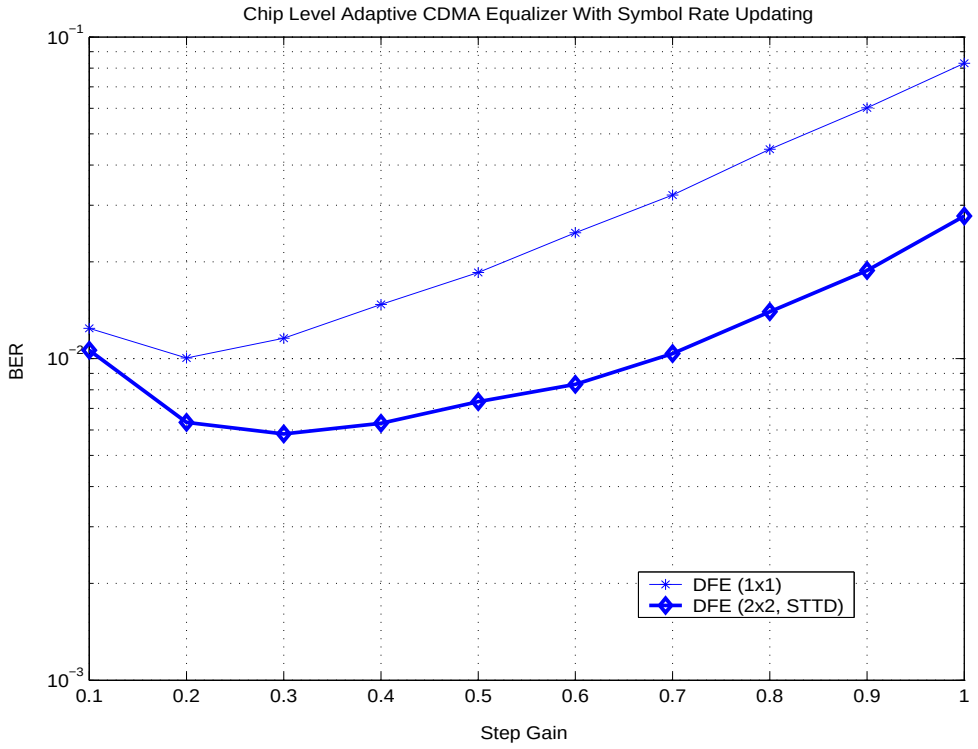

Figure 4.5: BER performance of the chip level DFE based on the Alamouti scheme with respect to the adaptation gain using the NLMS adaptation algorithm

In Fig. 4.7 and Fig. 4.8, the BER performance with respect to the number of users using the NLMS and the RLS algorithms is shown. The performance for all receivers deteriorates as the number of users becomes larger. Since the chip level DFE can suppress ICI more

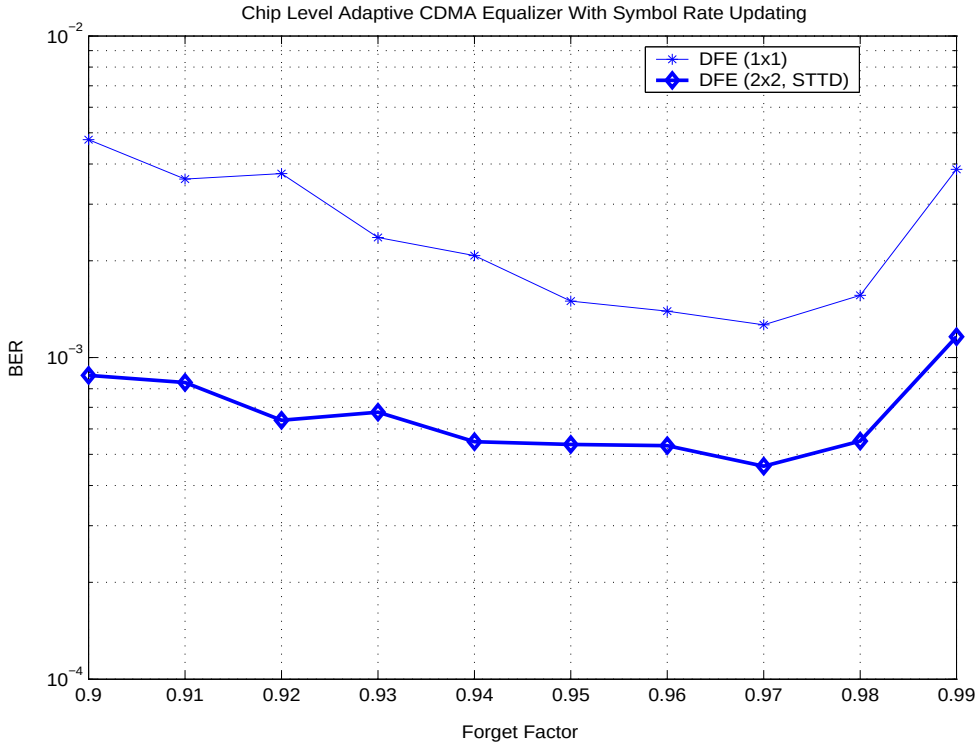

Figure 4.6: BER performance of the chip level DFE based on the Alamouti scheme with respect to the forgetting factor using the RLS adaptation algorithm

efficiently, it is less affected by MAI. Therefore, when the number of users increases, the performance of the chip level DFE would degrade less than that of the rake receiver. In addition, when the RLS algorithm is used, a significant improvement has been made, especially for the larger number of users. Additional BER improvement can also be made when multiple antennas are used.

The BER results are shown in Fig. 4.9 and Fig. 4.10 for various values of SNR using the NLMS and the RLS algorithms, respectively. Note that when the SNR is low, the noise is more dominant than MAI and the diversity gain is the key to provide better BER performance. Since the rake receiver with multiple antennas can exploit diversity gain, it can have good performance at low SNR.

At higher SNR, MAI becomes dominant. The chip level DFE can suppress MAI and it is less affected by MAI than the rake receiver. Thus, when the SNR becomes higher, the chip

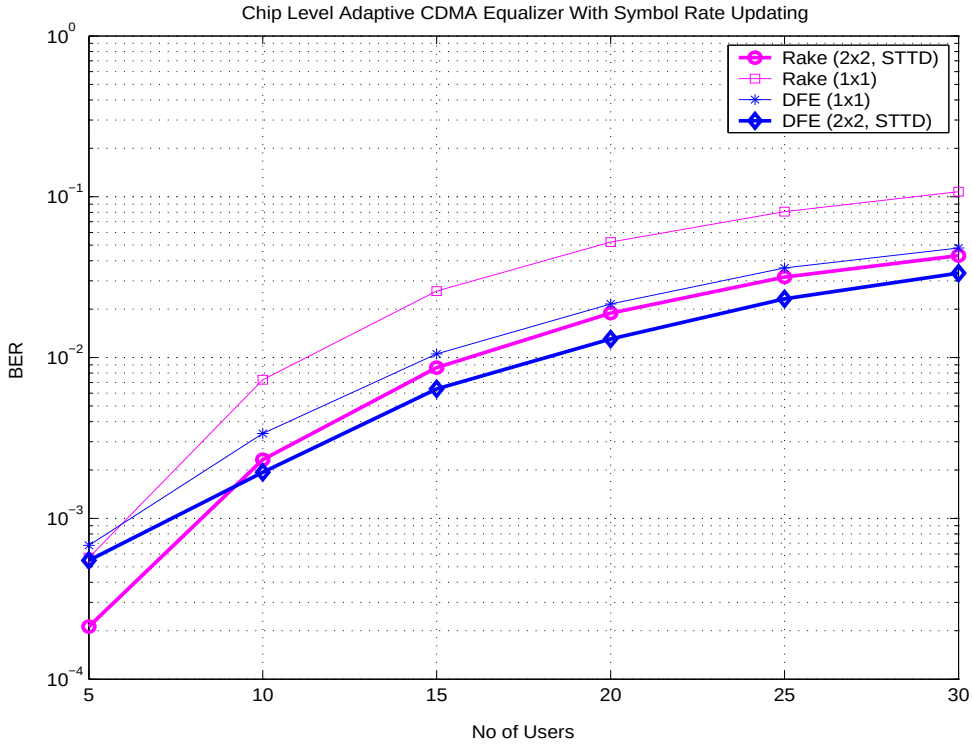

Figure 4.7: BER performance of the chip level DFE based on the Alamouti scheme with respect to the number of users using the NLMS adaptation algorithm

level DFE performs much better than the rake receiver. The improvement at different SNR level for the chip level DFE is also made when the RLS algorithm is used.

Fig. 4.7, Fig. 4.9 and Fig. 4.11 also show that the rake receiver can have a better combining gain compared to the chip level DFE based on the Alamouti scheme. The chip level DFE needs to mitigate the ICI as well as combine signals coherently, while the rake receiver only needs to maximize the combining gain without mitigating the ICI. For example, at a BER of 10^{-2}, the rake receiver based on multiple antennas (two transmit and two receive antennas) can accommodate fifty percent more users, compared to the rake receiver based on single antenna. On the other hand, the chip level DFE based on the Alamouti scheme can only accommodate about twenty percent more users at the same bit error level, compared to the chip level DFE for single antenna.

In general, it is expected that the speed of the mobile can affect the performance of adaptive

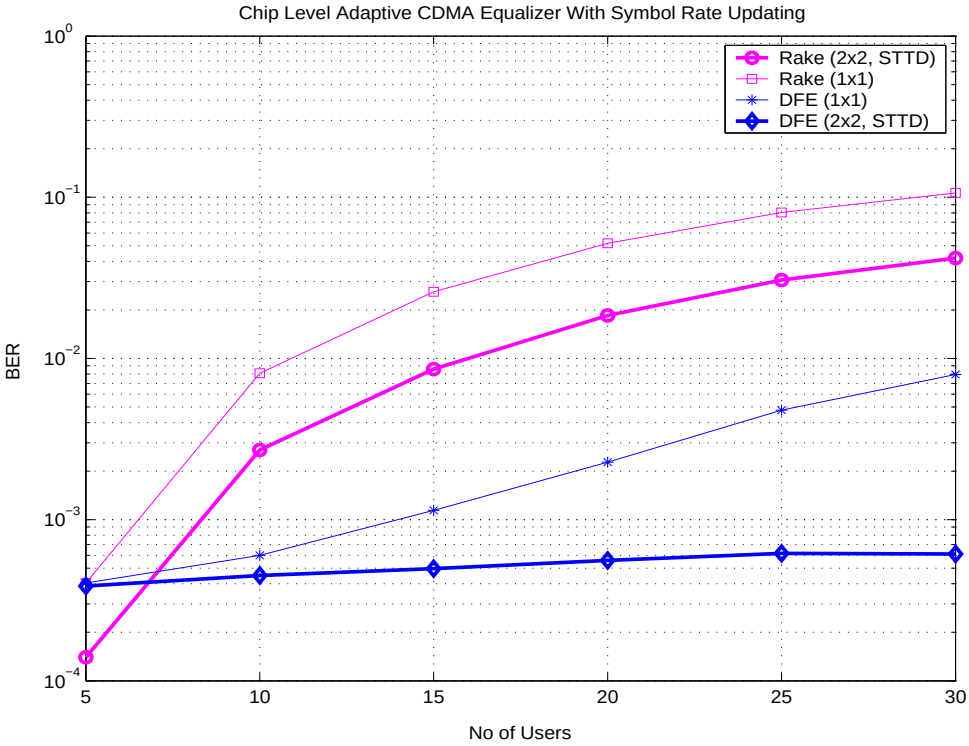

Figure 4.8: BER performance of the chip level DFE based on the Alamouti scheme with respect to the number of users using the RLS adaptation algorithm

equalization. Fig. 4.11 and Fig. 4.12 reveal that as the speed of the mobile becomes higher, it is more difficult for the equalizer to manage successfully the variation of channel. It results in the increase of MAI in the receivers. Consequently, the performance of the chip level DFE deteriorates as the speed of the mobile becomes higher. Note that the variation of the channel does not affect the performance of the rake receiver since the performance degradation is only due to the channel estimation error (we assume perfect CSI for the rake receiver).

4.4 Comparing Performance of the Chip Level DFE with the STS Scheme and the Alamouti Scheme

In Section 3.1 and Section 3.2, we have proposed the chip level DFE when the STS and the Alamouti scheme are employed in the transmitter. The theoretical analysis of the STS and

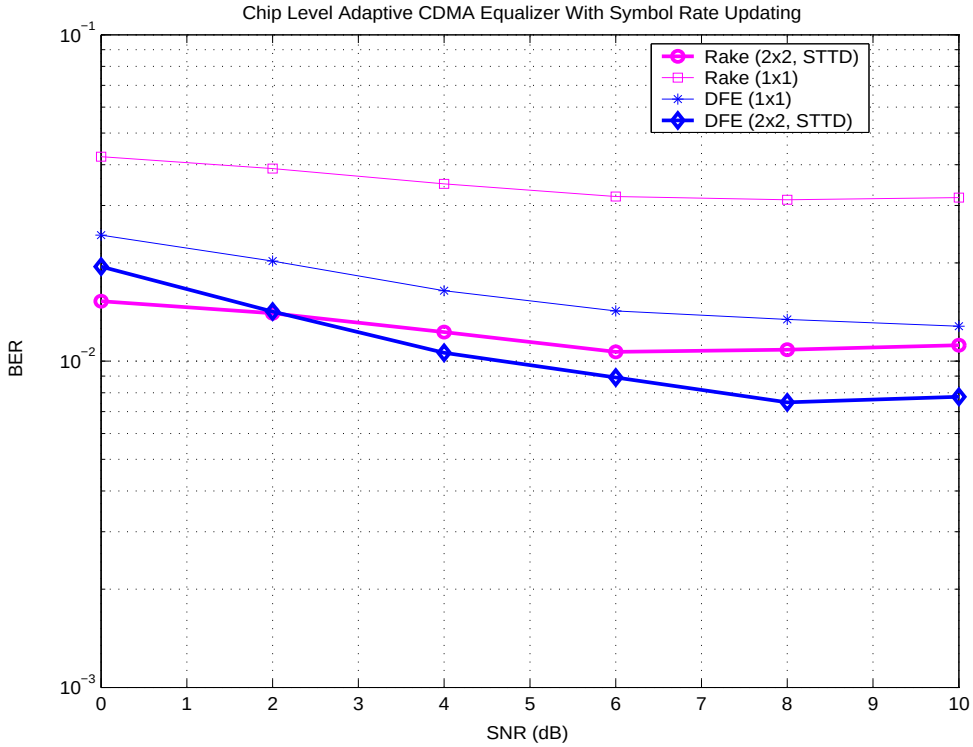

Figure 4.9: BER performance of the chip level DFE based on the Alamouti scheme with respect to SNR using the NLMS adaptation algorithm

the Alamouti schemes has also been presented in detail [26, 27].

Although the Alamouti scheme requires no extra spreading codes, both the Alamouti and the STS schemes can achieve the same diversity gain [26, 48]. The rake receiver exploits diversity gain to achieve better performance. Therefore, it can be expected that the rake receiver based on the STS and the Alamouti schemes can have approximately the same BER performance in multipath fading, as shown in Fig. 4.13.

Although the rake receiver can achieve approximately the same performance for both schemes, it is not the case for the chip level DFE, as shown in Fig. 4.13. In general, the equalization may not be perfect. It means that there still exists MAI at the output of the chip level DFE. The frequency selective fading causes more MAI for the chip level DFE with the Alamouti scheme. As a result, the performance of the chip level DFE based on the Alamouti scheme is worse than the chip level DFE based on the STS scheme.

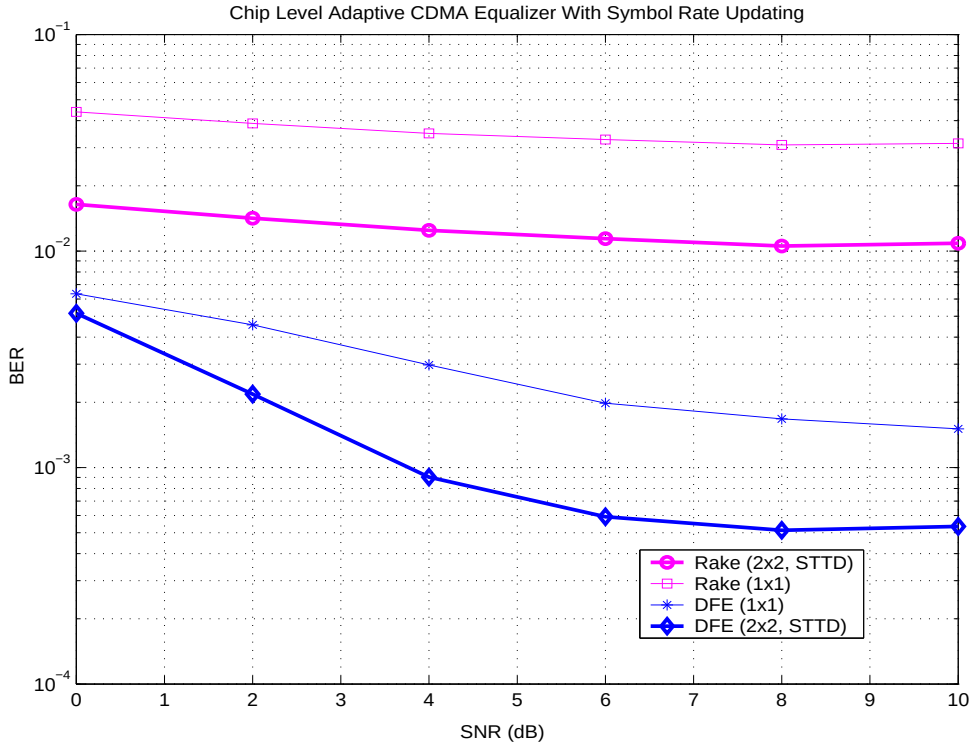

Figure 4.10: BER performance of the chip level DFE based on the Alamouti scheme with respect to SNR using the RLS adaptation algorithm

4.5 Comparing Performance of the Chip Level DFE using the NLMS Algorithm and the RLS Algorithm

Fig. 4.8, Fig. 4.10 and Fig. 4.12 show that the RLS adaptation algorithm can improve the performance significantly.

In time-variant frequency selective fading channel, a heavy load system (with larger number of users) causes more MAI at the receiver. The chip level equalizer using the simple NLMS algorithm cannot achieve its maximum performance in this situation since the equalizer also needs to cope with the changes and modify its coefficients. Therefore, a faster convergence rate is desired. Fig. 4.7 and Fig. 4.8 show that significant improvement is gained with the RLS algorithm, especially for higher number of users.

In general, the RLS algorithm has a smaller steady state error than the NLMS algorithm

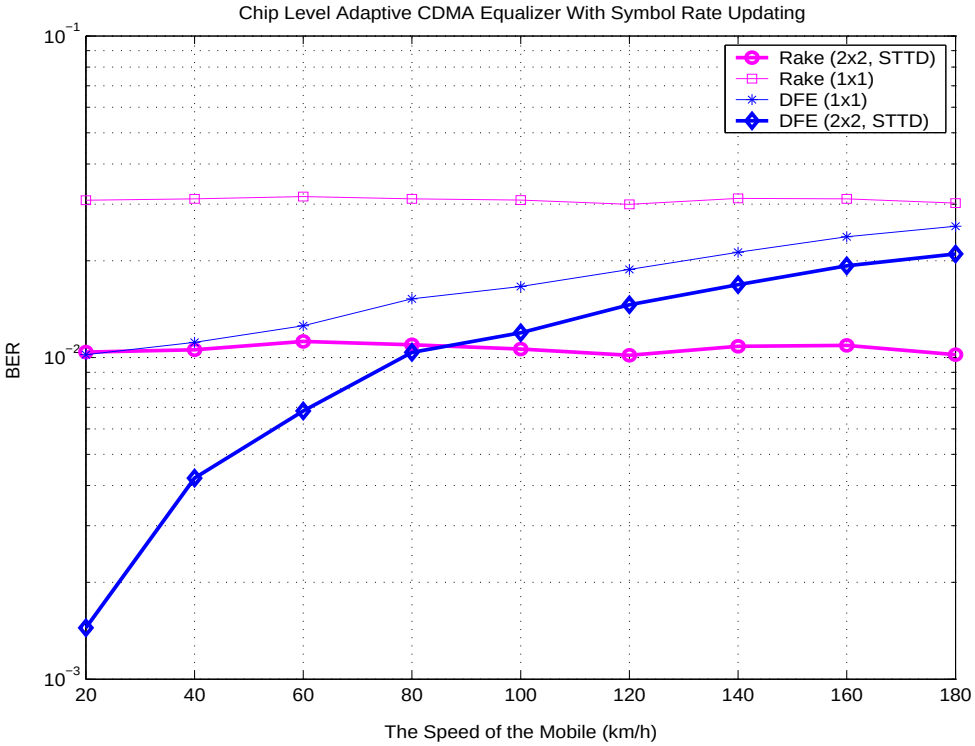

Figure 4.11: BER performance of the chip level DFE based on the Alamouti scheme with respect to the speed of the mobile using the NLMS adaptation algorithm

has. Consequently, BER performance is better in all circumstances. In addition, the RLS algorithm has a faster convergence rate, especially for higher SNR. Consequently, at higher SNR, the RLS algorithm can offer significant BER improvement, as shown in Fig. 4.9 and Fig. 4.10.

In general, it is expected that different adaptation algorithms can affect the BER performance of the chip level DFE on the different speed of the mobile, as shown in Fig. 4.11 and Fig. 4.12. As the speed of the mobile becomes higher, it is more difficult for the equalizer to cope with the variation of channel. Thus, there is a lot to gain by using a better adaptation algorithm. For example, at a BER of 10^{-2}, the chip level DFE (with multiple antennas) using the NLMS algorithm can outperform the rake receiver at speed below 85 km/hr. However, at the same bit error level, the chip level DFE using the RLS algorithm can outperform the rake receiver even when the speed of the user is 180 km/hr.

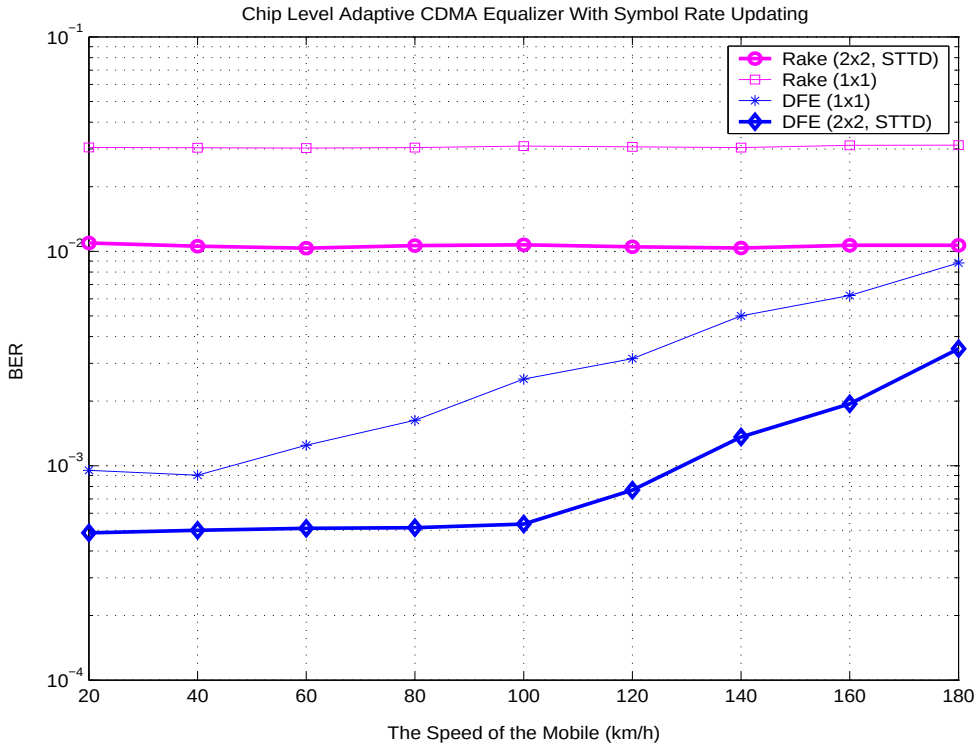

Figure 4.12: BER performance of the chip level DFE based on the Alamouti scheme with respect to the speed of the mobile using the RLS adaptation algorithm

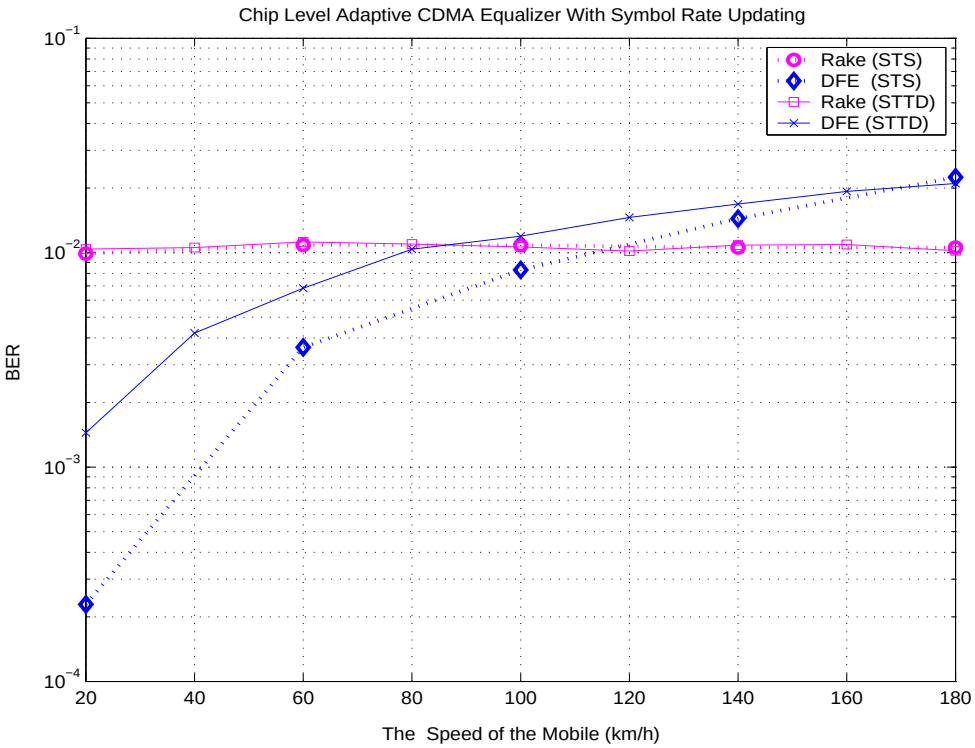

Figure 4.13: BER performance of the chip level DFE based on the STS scheme and the Alamouti scheme with respect to the speed of the mobile using the NLMS adaptation algorithm

Chapter 5

Conclusion and Further Research

5.1 Conclusion

This research study has demonstrated that significant improvement in performance and capacity can be made when the chip level DFE based on the STS scheme is used. The improvement can be achieved since the proposed receiver design exploits the diversity gain and suppresses the MAI at the same time. However, this receiver needs extra spreading codes.

We have proposed the chip level DFE for CDMA downlink channel when the Alamouti scheme is employed at the transmitter. Using an MMSE cost function, the optimal equalization vector and the closed form expression have also been obtained. It is shown that ICI of a channel and the interfering signal from the other transmit antennas can be suppressed simultaneously.

Comparing the performance of the chip level DFE in the STS scheme and the Alamouti scheme, the chip level DFE for CDMA downlink channel based on the Alamouti scheme has slightly worse performance than the chip level DFE based on the STS scheme. However, the Alamouti scheme does not require extra spreading codes.

It has been shown that the proposed method can restore the orthogonality on downlink chan-

nel and suppress MAI. In comparison with the rake receiver equipped with multiple antennas, the proposed method not only provides antenna diversity gain, but also suppresses MAI, while the rake receiver can only have antenna diversity gain. Hence, the proposed method can offer significant improvement in performance and capacity.

5.2 Further Research

The training (adaptation process) for the chip level DFE developed in this thesis is based on the pilot signals. If the channel is static, we can have sufficient samples (symbols) to find the equalization coefficients. When the channel is time-variant, only a few samples are available to track with the variation of channel. By utilizing the noise subspace from unused spreading sequences (blind technique), we can also have additional samples to find the equalization coefficients. Therefore, by utilizing both the pilot signal and unused spreading sequences (semiblind technique), we can improve the performance [49, 50]. Thus, the blind and semiblind techniques can be considered for the chip level DFE and it is an interesting future research topic.

In this thesis, the chip level based on the Alamouti scheme (two transmit antennas) has been developed. However, more general configuration with $I(> 2)$ transmit antennas can also be employed [28]. This can be considered as an extension of the current research.

The Alamouti scheme can achieve a maximum possible diversity advantage with a simple decoding algorithm. However, additional coding gain, spectral efficiency, and diversity improvement can be simultaneously obtained when space time trellis code (STTC) is used [51, 52]. The STTC with the chip level DFE can be integrated to have better performance. This can be considered as a further research issue.

Finally, in order to improve the capability of multimedia communications, W-CDMA can be designed to support a variety of data services from low to very high bit rates. Since the spreaded signal bandwidth is the same for all users, multiple rate transmission needs multiple

spreading factors. Therefore, another interesting research topic is the extension of the chip level DFE to the multiple spreading factor CDMA system.

Appendix A

Proof of the optimal solution for the conventional decision feedback equalizer under the mean square error criterion

Consider (2.16):

$$MSE = E\Big(|b[m] - \hat{b}[m]|^2\Big).$$

By using the principle of orthogonality [37], the MMSE solution of (2.16) can be written as:

$$E(\mathbf{d}[m]e^*[m]) = 0 \tag{1}$$

where $e[m] = b[m] - \hat{b}[m]$ is the error signal, $\mathbf{d}[m]$ is the complete received vector, and * is the complex conjugate operator.

If we substitute (2.13) and (2.14) into (1) and expand the equation, we can obtain:

$$E\Big\{ \begin{pmatrix} \mathbf{r}[m]\mathbf{r}^H[m] & -\mathbf{r}[m]\mathbf{b}^H[m] \\ -\mathbf{b}[m]\mathbf{r}^H[m] & \mathbf{b}[m]\mathbf{b}^H[m] \end{pmatrix} \Big\} \begin{pmatrix} \mathbf{c} \\ \mathbf{g} \end{pmatrix} = E\Big\{ \begin{pmatrix} \mathbf{r}[m]\mathbf{b}^*[m] \\ -\mathbf{b}[m]\mathbf{b}^*[m] \end{pmatrix} \Big\}. \tag{2}$$

Let us assume that the complex channel is time-invariant, i.e. $h[p;m] = h[p]$ for all p. Then, from (2.2) and (2.11), (2.10) can be written as:

$$\mathbf{r}[m] = \begin{pmatrix} \bar{\mathbf{H}}^H & \mathbf{H}^H \end{pmatrix} \begin{pmatrix} \bar{\mathbf{b}}[m] \\ \mathbf{b}[m] \end{pmatrix} + \begin{pmatrix} \eta[m+N_f] \\ \vdots \\ \eta[m] \end{pmatrix} \tag{3}$$

where

$$\mathbf{H} = \begin{pmatrix} h[N_f+1] & \dots & h[2] & h[1] \\ \vdots & & \vdots & \vdots \\ 0 & & h[N_b] & h[N_b-1] \\ 0 & \dots & 0 & h[N_b] \end{pmatrix}$$

$$\bar{\mathbf{H}} = \begin{pmatrix} h[0] & 0 & \dots & 0 \\ h[1] & h[0] & & 0 \\ \vdots & \vdots & \ddots & \vdots \\ h[N_f] & h[N_f-1] & \dots & h[0] \end{pmatrix}$$

$$\bar{\mathbf{b}}[m] = \begin{pmatrix} b[m+N_f] \\ \vdots \\ b[m] \end{pmatrix}.$$

Assume that the noise and the symbol sequences are uncorrelated, i.e. $E(b[m]\eta[m]) = 0$. If we substitute (3) into (2), expand the equation, and equate the left hand and right hand equation, we can obtain:

$$\begin{aligned} \mathbf{g} &= \mathbf{Hc} \\ \mathbf{c} &= (\bar{\mathbf{H}}^H \bar{\mathbf{H}} + \sigma_n^2 \mathbf{I})^{-1} \mathbf{h}_c^* \end{aligned}$$

where $\mathbf{h}_c^T$ is the (N_f+1) row vector of matrix $\bar{\mathbf{H}}$, $\mathbf{I}$ is the identity matrix, and $E[|\eta[m]|^2] = \sigma_n^2$. It completes the proof.

Appendix B

Proof of the closed form solution of optimal equalization vector for the Alamouti scheme

Consider (3.25):

$$\begin{aligned} \mathbf{\Omega}[n] &= \sum_{i=1}^{2} \bar{\mathbf{H}}_i^H \bar{\mathbf{u}}^{(i)}[n] + \bar{\mathbf{n}}[n] \\ \mathbf{u}[n-D-1] &= \begin{pmatrix} u^{(1)}[n-D-1] \\ \vdots \\ u^{(1)}[n-D-N_b] \\ u^{(2)}[n-D-1] \\ \vdots \\ u^{(2)}[n-D-N_b] \end{pmatrix}. \end{aligned}$$

For $i = 1, 2$, let us define:

$$\bar{A} = \bar{A}_i \tag{4}$$

$$P_s = \sum_{k=1}^{K} |A_k|^2 \tag{5}$$

$$\beta = \frac{P_s + |\bar{A}|^2}{N} \sigma_b^2 \tag{6}$$

$$\mathbf{R}_{11} = \beta \sum_{i=1}^{2} \bar{\bar{\mathbf{H}}}_i^H \bar{\bar{\mathbf{H}}}_i + |\bar{A}|^2 \sigma_b^2 (\bar{\mathbf{H}}_i)_{D+1}^H (\bar{\mathbf{H}}_i)_{D+1} + \sigma_n^2 \mathbf{I} \tag{7}$$

where $\mathbf{I}$ is the identity matrix, $(\cdot)_{D+1}$ indicates the $(D+1)$th row of the corresponding matrix, $\bar{\bar{\mathbf{H}}}_i$ is the matrix which is obtained from $\bar{\mathbf{H}}_i$ with removing the $(D+1)$th row vector, σ_b^2 is the variance of data symbol, σ_n^2 is the noise variance, and $\bar{A}$ is the amplitude of the pilot signal.

Under **A1**, **A2**, and **A3**, we have

$$E(\sum_{l=0}^{N-1} \mathbf{\Omega}[mN+l+D]\bar{s}^{*(i)}[mN+l]\bar{b}^{*(i)}[m]) = \bar{A}\sigma_b^2(\bar{\mathbf{H}}_i)_{D+1}^H \quad (8)$$

$$E(\sum_{l=0}^{N-1} \mathbf{u}[mN+l-1]\bar{s}^{*(i)}[mN+l]\bar{b}^{*(i)}[m]) = \mathbf{0} \quad (9)$$

$$E(\sum_{l=0}^{N-1}\sum_{l'=0}^{N-1} \mathbf{\Omega}[mN+l+D]\bar{s}^{*(i)}[mN+l]\bar{s}^{(i)}[mN+l']\mathbf{\Omega}^H[mN+l'+D]) = \mathbf{R}_{11} \quad (10)$$

$$E(\sum_{l=0}^{N-1}\sum_{l'=0}^{N-1} \mathbf{\Omega}[mN+l+D]\bar{s}^{*(i)}[mN+l]\bar{s}^{(i)}[mN+l']\mathbf{u}^H[mN+l'-1]) = \beta\begin{pmatrix} (\bar{\mathbf{H}}_1)_{D+2:D+N_b+1} \\ (\bar{\mathbf{H}}_2)_{D+2:D+N_b+1} \end{pmatrix}^H \quad (11)$$

$$E(\sum_{l=0}^{N-1}\sum_{l'=0}^{N-1} \mathbf{u}[mN+l-1]\bar{s}^{*(i)}[mN+l]\bar{s}^{(i)}[mN+l']\mathbf{\Omega}^H[mN+l'+D]) = \beta\begin{pmatrix} (\bar{\mathbf{H}}_1)_{D+2:D+N_b+1} \\ (\bar{\mathbf{H}}_2)_{D+2:D+N_b+1} \end{pmatrix} \quad (12)$$

$$E(\sum_{l=0}^{N-1}\sum_{l'=0}^{N-1} \mathbf{u}[mN+l-1]\bar{s}^{*(i)}[mN+l]\bar{s}^{(i)}[mN+l']\mathbf{u}^H[mN+l'-1]) = \beta\mathbf{I} \quad (13)$$

where **0** is the null matrix and $(\cdot)_{D+2:D+N_b+1}$ indicates rows $(D+2)$ to $(D+N_b+1)$.

Let us also recall (3.30) and rewrite for convenience.

$$\begin{aligned} \mathbf{w}_i &= \frac{E\big(\sum_{l=0}^{N-1} \mathbf{d}[mN+l+D]\bar{s}^{*(i)}[mN+l]\bar{b}^{*(i)}[m]\big)}{E\big(\sum_{l=0}^{N-1}\sum_{l'=0}^{N-1} \mathbf{d}[mN+l+D]\bar{s}^{*(i)}[mN+l]\bar{s}^{(i)}[mN+l']\mathbf{d}^H[mN+l'+D]\big)} \\ \mathbf{d}[n] &= (\mathbf{\Omega}^T[n] \quad -\mathbf{u}^T[n-D-1])^T. \end{aligned}$$

If we substitute (8) - (13) into (3.30), we are able to obtain:

$$\mathbf{w}_i = \begin{pmatrix} \mathbf{c}_i \\ \mathbf{g}_i \end{pmatrix} = \mathbf{R}^{-1}\mathbf{p}_i \qquad i = 1, 2$$

where

$$\begin{aligned} \mathbf{p}_i &= \bar{A}\sigma_b^2 \begin{pmatrix} (\bar{\mathbf{H}}_i)_{D+1}^H \\ \mathbf{0} \end{pmatrix} \\ \mathbf{R} &= \beta \begin{pmatrix} \frac{\mathbf{R}_{11}}{\beta} & -(\bar{\mathbf{H}}_1)_{D+2:D+N_b+1}^H & -(\bar{\mathbf{H}}_2)_{D+2:D+N_b+1}^H \\ -(\bar{\mathbf{H}}_1)_{D+2:D+N_b+1} & \mathbf{I} & \mathbf{0} \\ -(\bar{\mathbf{H}}_2)_{D+2:D+N_b+1} & \mathbf{0} & \mathbf{I} \end{pmatrix} \end{aligned}$$

It completes the proof.

Bibliography

[1] J. Geier, "Benefits of wireless networks," *Wireless-Nets Consulting Services*, Aug. 2000.

[2] T. S. Rappaport, *Wireless Communications*, Prentice Hall, New Jersey, 1996.

[3] S. Haykin, *Communication Systems*, Wiley, 4th edition, 2001.

[4] M. Mouly and M. B. Pautet, *The GSM System for Mobile Communications*, Kluwer Academic Publishers, Palaiseau, 1992.

[5] T. Ojanpera and R. Prasad, *Wideband CDMA for Third Generation Mobile Communications*, Artech House Boston, 1998.

[6] G. Leus, *Signal Processing Algorithms for CDMA-Based Wireless Communications*, Ph.D. thesis, Departement Elektrotechniek, Faculteit Der Toegepaste Wetenschappen, Katholieke Universiteit Leuven, May 2000.

[7] R. Price and P. E. Green, "A communication technique for multipath channels," in *Proc. IRE*, Mar. 1958, vol. 46, pp. 555–570.

[8] S. Verdu, *Multiuser Detection*, Cambridge University Press, New York, NY, 1998.

[9] R. Lupas and S. Verdu, "Near-far resistance of multiuser detectors in asynchronous channels," *IEEE Trans. Commun.*, vol. 38, no. 4, pp. 496–508, Apr. 1990.

[10] Z. Xie, R.T. Short, and C. K. Rushforth, "A family of suboptimum detectors for coherent multiuser communications," *IEEE J. Select. Areas Commun.*, vol. 8, no. 4, pp. 683–690, May 1990.

[11] R. Kohno, H. Imai, M. Hatori, and S. Pasupathy, "Combination of an adaptive array antenna and a canceller of interference for direct-sequence spread-spectrum multiple-access system," *IEEE J. Select. Areas Commun.*, vol. 8, no. 4, pp. 675–682, May 1990.

[12] C.D. Frank and E. Visotsky, "Adaptive interference suppression for the downlink of a direct sequence CDMA system with long spreading codes," in *Proc. 36th Allerton Conf. on Comm., Contr. and Comp.*, Monticello, IL, Sept. 1998.

[13] K. Hooli, M. Latva-Aho, and M. Juntti, "Multiple access interference suppression with linear chip equalizers in WCDMA downlink receivers," in *Proc. IEEE Global Telecommunications Conf.*, Rio de Janeiro, Brazil, Dec. 1999, vol. General Conference (Part A), pp. 467–471.

[14] F. Petre, M. Moonen, M. Engels, B. Gyselinckx, and H. D. Man, "Pilot-aided adaptive chip equalizer receiver for interference suppression in DS-CDMA forward link," in *Proc. IEEE Int. Vehicular Technology Conf.*, Boston, MA, Sept. 2000, vol. I, pp. 303–308.

[15] J. Choi, "MMSE equalization of downlink CDMA channel utilizing unused orthogonal spreading sequences," *IEEE Trans. Signal Processing*, vol. 51, no. 5, pp. 1390–1402, May 2003.

[16] M.E. Austin, "Decision-feedback equalization for digital communication over dispersive channels," *M.I.T. Lincoln Laboratory*, Aug. 1967.

[17] J. Salz, "Optimum mean square decision feedback equalization," *Bell System Technology Journal*, vol. 53, no. 8, pp. 1341–1373, Oct. 1973.

[18] N. Al-Dhahir and J.M. Cioffi, "MMSE decision-feedback sequence estimation," *IEEE Trans. Inform. Theory*, vol. 41, pp. 961–975, July 1995.

[19] J. G. Proakis, *Digital Communications*, McGraw Hill International, 4th edition, 2000.

[20] M. Abdulrahman, A.U.H. Sheikh, and D.D. Falconer, "Decision feedback equalization for CDMA in indoor wireless communication," *IEEE J. Select. Areas Commun.*, vol. 12, pp. 698–706, May 1994.

[21] J.E. Smee and S.C. Schwartz, "Adaptive feedforward feedback architectures for multiuser detection in high data rate wireless CDMA networks," *IEEE Trans. Commun.*, vol. 48, pp. 996–1011, June 2000.

[22] J.F. Robler, L.H.J. Lampe, W.H. Gerstacker, and J.B. Huber, "Decision feedback equalization for CDMA downlink," in *Int. Vehicular Technology Conf.*, Spring 2002, vol. 2, pp. 816–820.

[23] E. Telatar, "Capacity of multi-antenna Gaussian channels," Tech. memo., AT&T Bell Labs, June 1995.

[24] G.J. Foschini and M.J. Gans, "On the limits of wireless communications in a fading environment when using multiple antennas," *Wireless Pers. Commun.*, vol. 6, no. 3, pp. 311–335, Mar. 1998.

[25] A.F. Naguib, N. Seshadri, and A.R. Calderbank, "Increasing data rate over wireless channel," *IEEE Signal Processing Mag.*, pp. 76–92, May 2000.

[26] B. Hochwald, T.L. Marzetta, and C.B. Papadias, "A transmitter diversity scheme for wideband CDMA systems based on space-time spreading," *IEEE J. Select. Areas Commun.*, vol. 19, pp. 48–60, Jan. 2001.

[27] S.M. Alamouti, "A simple transmit diversity technique for wireless communication," *IEEE J. Select. Areas Commun.*, vol. 16, pp. 1451–1458, Oct. 1998.

[28] V. Tarokh, H. Jafarkhani, and A. Calderbank, "Space-time block codes from orthogonal designs," *IEEE Trans. Inform. Theory*, vol. 45, pp. 1456–1467, July 1999.

[29] A. Duel-Hallen, "Equalizers for multiple input multiple output channels and PAM systems with cyclostationary input sequences," *IEEE J. Select. Areas Commun.*, vol. 10, no. 3, pp. 630–639, Apr. 1992.

[30] N. Al-Dhahir, A.F. Naguib, and A.R. Calderbank, "Finite-length MIMO decision feedback equalization for space-time block-coded signals over multipath fading channels," *IEEE Trans. Veh. Technol.*, vol. 50, no. 4, pp. 1176 –1182, July 2001.

[31] A. Lozano and C. Papadias, "Layered space-time receivers for frequency selective wireless channels," *IEEE Trans. Commun.*, vol. 50, no. 1, pp. 65–73, Jan. 2002.

[32] F. Petre, G. Leus, L. Deneire, M. Engels, and M. Moonen, "Adaptive space-time chip equalization for WCDMA downlink with code-multiplexed pilot and soft handover," in *Proc. IEEE Int. Conf. Communications*, May 2002, vol. 3, pp. 1635–1639.

[33] G. Leus, F. Petre, and M. Moonen, "Space-time chip equalization for space time coded downlink CDMA," in *Proc. IEEE Int. Conf. Communications*, May 2002, vol. 1, pp. 568–572.

[34] A.J. Paulraj, "Space time processing for wireless communications," *IEEE Signal Processing Mag.*, pp. 49–83, Nov. 1997.

[35] R.D. Gitlin, J.F. Hayes, and S.B. Weinstein, *Data Communications Principles*, Plenum Press, New York and London, 1992.

[36] E. A. Lee and D. G. Messerschmitt, *Digital Communication*, Kluwer Academic Publishers, Boston, 1988.

[37] S. Haykin, *Adaptive Filter Theory*, Prentice Hall International, New Jersey, 3rd edition, 1996.

[38] A. J. Viterbi, *CDMA: Principles of Spread Spectrum Communication*, Addison-Wesley, Pub. Reading, MA, 1995.

[39] M. Latva-aho and M. Juntti, "Adaptive LMMSE-RAKE receiver for DS-CDMA systems," in *URSI/IEEE/INFOTECH XXII Convention on Radio Science*, Oulu, Finland, Nov. 1997, pp. 51–52.

[40] J. Ramos, M.D. Zoltowski, and H. Liu, "A low complexity space time rake receiver for DS-CDMA communication," *IEEE Signal Processing Lett.*, vol. 4, no. 9, pp. 262–265, Sept. 1997.

[41] A. Klein, "Data detection algorithms specially designed for the downlink of CDMA mobile radio systems," in *Proc. IEEE Int. Vehicular Technology Conf.*, Phoenix, AZ, May 1997, pp. 203–207.

[42] I. Ghauri and D. Slock, "Linear receivers for the DS-CDMA downlink exploiting orthogonality of spreading sequences," in *Proc. 32nd Asilomar Conference on Signals, Systems and Computers*, Nov. 1998, pp. 650–654.

[43] S. Werner and J. Lilleberg, "Downlink channel decorrelation in CDMA systems with long codes," in *Proc. IEEE Int. Vehicular Technology Conf.*, Houston, TX, May 1999, pp. 1614–1617.

[44] P. Komulainen, M.J. Heikkila, and J. Lilleberg, "Adaptive channel equalization and interference suppression for CDMA downlink," in *Proc. IEEE Int. Symp. Spreading Spectrum Techniques and Applications*, NJ, Sept. 2000, pp. 363–367.

[45] T.P. Krauss and M.D. Zoltowski, "Chip level MMSE equalization at the edge of the cell," in *Proc. IEEE Wireless Communications and Networking Conf.*, Chicago,IL, Sept. 2000, pp. 23–28.

[46] S. Chowdhury and M.D. Zoltowski, "Adaptive MMSE equalization for wideband CDMA forward link with time-varying frequency selective channels," in *Proc. IEEE Int. Conf. on Accoustics, Speech, and Signal Processing*, May 2002, vol. 3, pp. 2609–2612.

[47] 3GPP, *Physical Layer Procedures (FDD)*, Tech. Rep., Jun. 1999.

[48] G. Wu, H. Wang, M. CHen, and S. Cheng, "Performance comparison of space-time spreading and space-time transmit diversity in CDMA 2000," in *Int. Vehicular Technology Conf.*, Fall 2001, vol. 1, pp. 442–446.

[49] K. Li and H. Liu, "A new blind receiver for downlink DS-CDMA communications," *IEEE Commun. Lett.*, vol. 3, no. 7, pp. 193–195, July 1999.

[50] D.T.M. Slock and I. Ghauri, "Blind maximum SINR receiver for the DS-CDMA downlink," in *Proc. IEEE Int. Conf. on Accoustics, Speech, and Signal Processing*, Istambul, Turkey, June 2000, pp. 2485 – 2488.

[51] V. Tarokh, N. Seshadri, and A. Calderbank, "Space-time codes for high data rate wireless communication: Performance criterion and code construction," *IEEE Trans. Inform. Theory*, vol. 44, no. 2, pp. 744–765, Mar. 1998.

[52] Z. Chen, J. Yuan, and B. Vucetic, "Improved space-time trellis coded modulation scheme on slow Rayleigh fading channels," *IEE Electron. Lett.*, vol. 37, pp. 440–441, Mar. 2001.